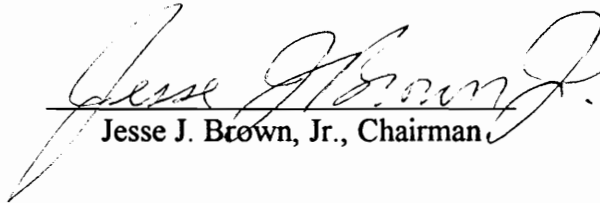


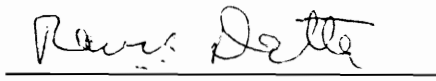
**COMPOSITION MODIFICATION OF ZINC TITANATE ( $Zn_2TiO_4$ )  
BASED SORBENTS FOR HOT COAL GAS DESULFURIZATION**

by  
Kimberly S. Walton

Thesis submitted to the Faculty of the  
Virginia Polytechnic Institute and State University  
in partial fulfillment of the requirements for the degree of  
**MASTER OF SCIENCE**  
in  
Materials Science and Engineering

APPROVED:

  
Jesse J. Brown, Jr., Chairman

  
Ranajit K. Datta

  
Gerald H. Luttrell

September 1995  
Blacksburg, Virginia

Keywords: Zinc Titanate, Spinel, Desulfurization, Sorbents, Coal Gas Cleanup

**COMPOSITION MODIFICATION OF ZINC TITANATE ( $Zn_2TiO_4$ ) BASED  
SORBENTS FOR HOT COAL GAS DESULFURIZATION**

by

Kimberly S. Walton

Committee Chairman: Jesse J. Brown, Jr.

Materials Science and Engineering

**(ABSTRACT)**

Advanced power generation systems require regenerable sorbents capable of removing sulfur from coal gas to low ppm levels. Zinc titanate ( $Zn_2TiO_4$ ) based sorbents are currently the leading sorbent for sulfur removal at high temperatures ( $\sim 700^\circ C$ ). Zinc titanate sorbents are still in need of development to address the problems of zinc vaporization, physical degradation, and low attrition resistance during the many sulfidation and regeneration cycles.

Based on the principles of phase equilibria and crystal chemistry, the approach being investigated in this project to eliminate these problems with zinc titanate sorbents is incorporation of various cations into the  $Zn_2TiO_4$  spinel structure. The study involved synthesis, characterization, and evaluation of the modified  $Zn_2TiO_4$  sorbents at the lab-scale size. Samples were characterized by XRD and TGA under simulated coal gas and an  $H_2S$  gas mixture to 1) determine the solid solubility of five cations (Ni, Cr, Al, Mg, and Cu) in the  $Zn_2TiO_4$  lattice and 2) determine the effect of the cations on the sulfur removal performance of  $Zn_2TiO_4$  sorbents.

The five cations selected were incorporated into the  $Zn_2TiO_4$  lattice in significant amounts, up to ~35 mole percent for Ni, Cr, Cu, and Al and ~25 mole percent for Mg at 1100°C. Based on the high chemical reactivity and durability observed in preliminary screening, Cr-incorporated  $Zn_2TiO_4$  sorbents, with compositions ranging from 3 to 35 mole percent Cr, were selected for further testing and characterization, including XRD, TGA, crush strength, and EDX. No correlation was found between Cr concentration and porosity, crush strength, and weight gain (sulfur removal). Cr-incorporated sorbents reduced Zn losses from 16.4% with 22.2 mole percent to 1.2% loss with 26.1 mole percent Cr.

## ACKNOWLEDGMENTS

I would like to thank Dr. Ran Datta for the year of patience, guidance, numerous discussions, and encouragement that has enabled me to complete this project. I would also like to thank Dr. Jesse Brown and Dr. Gerry Luttrell for serving on my committee.

I want to thank Dr. James Swisher and Mr. Jing Yang from SIUC for help with TGA and crush strength tests. Thanks also to Dr. R. Gupta at Research Triangle Institute for testing samples.

I want to recognize the sponsors of this project including the Illinois Clean Coal Institute and Department of Energy and also the Materials Science and Engineering Department for their financial assistance.

Several people deserve special recognition for their patience in helping me: J. K. Chen for helping me with computers and having answers for all of my questions: Jan Doran for helping with administrative details as well as providing support and encouragement through the tough times.

I could not have made it through the last few years without my good friends Jud Marte, Heidi Allison, and Steve Kan. Thanks for putting up with me, helping me maintain my sanity, and giving me so many great times and memories. Thanks also to Eric Wuchina for reviewing my thesis and being a great friend. There are others who have been there along the way including Oakey, Scott, Mike, Sherry, Levon, Becky, Drew and many more who made my years at Tech memorable.

Finally and most importantly, I wish to thank my family. There are not enough words to say how much I appreciate my parents, Todd, and Heather for their love and support, especially over the past six years. I would not have gotten this far without them and I will always be grateful.

# TABLE OF CONTENTS

Page Number

<b>ABSTRACT</b>	ii
<b>ACKNOWLEDGMENTS</b>	iv
<b>LIST OF FIGURES</b>	viii
<b>LIST OF TABLES</b>	x
<b>1.0 INTRODUCTION AND BACKGROUND</b>	
1.1 Introduction	1
1.2 Coal Formation	2
1.3 Desulfurization Principles	3
1.4 Background of Sorbent Compositions	8
1.5 Zinc Titanate System	10
<b>2.0 OBJECTIVES AND APPROACH</b>	
2.1 Objectives	13
2.2 Crystal Chemistry of Spinel	14
2.3 Cation Selection	18
<b>3.0 EXPERIMENTAL PROCEDURE</b>	
3.1 Sample Preparation	
3.1.1 Powder Synthesis	24
3.1.2 Pellet Preparation	25
3.1.2.1 Large Particle Size ZnO and TiO <sub>2</sub>	25
3.2 Characterization	
3.2.1 XRD Analysis	26
3.2.2 Density and Porosity Measurements	26
3.2.3 Stability of Cr-Incorporated Sorbents	27
3.2.4 Crush Strength Determination	27
3.2.5 Thermogravimetric Analysis	
3.2.5.1 Testing at Southern Illinois University at Carbondale	28
3.2.5.2 Testing at Research Triangle Institute	30
3.2.6 EDX Analysis	30
<b>4.0 EXPERIMENTAL RESULTS AND DISCUSSION</b>	
4.1 Solubility Range Determination for All Selected Cations	32
4.2 ZnO - TiO <sub>2</sub> - Cr <sub>2</sub> O <sub>3</sub> System	35

4.2.1 Mode of Substitution	36
4.3 Sulfidation and Regeneration	
4.3.1 Stability of Sorbents at Sulfidation Temperatures	40
4.3.2 XRD	40
4.3.3 Density, Porosity, and Crush Strength Measurements	42
4.3.4 TGA from SIUC	42
4.3.5 TGA from RTI	53
4.3.6 EDX Analysis	53
<b>5.0 SUMMARY AND CONCLUSIONS</b>	<b>57</b>
<b>REFERENCES</b>	<b>60</b>
<b>APPENDICES</b>	
Appendix A	64
Appendix B	65
Appendix C	70
<b>VITA</b>	<b>71</b>

## LIST OF FIGURES

Page #

- Figure 1.1 Schematic diagram of the desulfurization process. [16] 6
- Figure 2.1 Spinel structure. [37] 16
- Figure 2.2 Theoretical weight gain of completely sulfided  $Zn_2TiO_4$  with increasing additions of Cr. 22
- Figure 4.1 Change in lattice parameter of the spinel phase for  $Zn_{2-x}M_{2x}Ti_{1-x}O_4$ , M= Cr or Al at a) 1000°C and b) 1000°C. 33
- Figure 4.2 Change in lattice parameter of the spinel phase for  $Zn_{2-x}M_xTiO_4$ , M=Ni, Mg, or Cu at a) 1000°C and b) 1000°C. 34
- Figure 4.3 Phase diagram for the ZnO - TiO<sub>2</sub> - Cr<sub>2</sub>O<sub>3</sub> system showing the modes of substitution. 37
- Figure 4.4 Trends in the change of lattice parameter of the spinel phase with mode of substitution. 39
- Figure 4.5  $Zn_{1.9}Ti_{0.9}Cr_{0.2}O_4$  sintered at 900°C for 3 hours a) sulfidation in 0.9%H<sub>2</sub>S, 92.4%H<sub>2</sub>, and 6.7%N<sub>2</sub> at 650°C and b) regeneration in 5%O<sub>2</sub> and 95%N<sub>2</sub> at 650°C. 45
- Figure 4.6  $Zn_{1.8}Ti_{0.8}Cr_{0.4}O_4$  sintered at 900°C for 3 hours a) sulfidation in 0.9%H<sub>2</sub>S, 92.4%H<sub>2</sub>, and 6.7%N<sub>2</sub> at 650°C and b) regeneration in 5%O<sub>2</sub> and 95%N<sub>2</sub> at 650°C. 46
- Figure 4.7 Sulfidation in 0.9%H<sub>2</sub>S, 92.4%H<sub>2</sub>, and 6.7%N<sub>2</sub> at 650°C and regeneration in 5%O<sub>2</sub> and 95%N<sub>2</sub> at 650°C of  $Zn_{1.95}Ti_{0.95}Cr_{0.1}O_4$  sintered at 900°C for 3 hours. 47
- Figure 4.8 Sulfidation in simulated coal gas at 650°C of a) 56.5ZnO-15Cr<sub>2</sub>O<sub>3</sub>-28.5TiO<sub>2</sub> (mole percent) and b) 55ZnO-25Cr<sub>2</sub>O<sub>3</sub>-20TiO<sub>2</sub> (mole percent). 48
- Figure 4.9 Sulfidation of  $Zn_{1.6}Cr_{0.4}TiO_{4.2}$  sintered at 950°C for 3 hours in a) simulated coal gas at 650°C and b) 0.9%H<sub>2</sub>S, 92.4%H<sub>2</sub>, and 6.7%N<sub>2</sub> at 650°C. 50
- Figure 4.10 Sulfidation of  $Zn_{1.6}Cr_{0.4}TiO_{4.2}$  sintered at 950°C for 3 hours in simulated coal gas at 725°C. 51

Figure 4.11 Initial Cr/Zn ratio versus Cr/Zn ratio after sulfidation at 650°C.

55

<b>LIST OF TABLES</b>	<b>Page #</b>
Table 1.1 Sulfur content in various coals from seams across the United States. [10]	4
Table 2.1 Site preference energies for various cations in spinels. [43]	17
Table 2.2 Ionic radii for ions used in this study. [41]	20
Table 3.1 Composition of simulated coal gas used in TGA studies at SIUC.	29
Table 3.2 Composition of gases used in TGA studies at RTI.	31
Table 4.1 Lattice parameter data for $Zn_{2-x}Cr_xTiO_4$ prepared at 1100°C and held for various times at 650°C.	41
Table 4.2 Density and porosity data for the Cr-incorporated sorbents.	43
Table 4.3 Crush strength measurements for the Cr-incorporated sorbents.	44
Table 4.4 Weight change after TGA tests for Cr-incorporated sorbents.	52
Table 4.5 Percent zinc loss after sulfidation of Cr-incorporated $Zn_2TiO_4$ sorbents.	56

# 1.0 INTRODUCTION AND BACKGROUND

## 1.1 Introduction

Coal represents 85% of the fossil fuel resources in the United States. [1] One of the primary concerns for coal-based power generation processes such as the Integrated Gasification Combined Cycle (IGCC) and the Molten Carbonate Fuel Cell (MCFC) is the emission of sulfur bearing volatiles causing environmental pollution and chemical corrosion to the turbine or fuel cell components. [2,3] These systems require removal of sulfur species ( $H_2S$  and  $COS$ ) from several hundred parts per million (ppm) to less than 10 ppm for IGCC and  $\sim 1$  ppm for MCFC. [4,5] Removal of sulfur to low levels also complies with the stricter environmental regulations, such as the Clean Air Act. [6] Highly efficient and cost effective methods are needed to convert coal into electricity in an environmentally acceptable way. Employing a solid, regenerable, mixed-metal oxide sorbent capable of sulfur removal at high temperatures ( $\sim 700^\circ C$ ) is one approach being studied to minimize the sulfur emission problem, increase the efficiency of the process, and lower material costs. [4,7,8,9]

Among the sorbents being investigated, pellets made of zinc oxide ( $ZnO$ ) and titania ( $TiO_2$ ) based compositions are currently the most promising in removing sulfur at high temperatures, and the spinel form zinc titanate ( $Zn_2TiO_4$ ) has been the candidate for recent investigations. However, problems with zinc losses and physical durability of the sorbent pellets over many sulfidation and regeneration cycles may limit its long term use

and increase the cost of the power generation process. Incorporating certain metal ions in the zinc titanate lattice is an approach being used to alleviate these concerns and improve the performance of zinc titanate sorbents.

## **1.2 Coal Formation**

Many coal deposits in the United States, such as Illinois basin coal, contain large quantities of sulfur. Coal is an organic rock originating from the slow decomposition and chemical conversion of immense masses of organic material through geological processes involving elevated temperatures, pressures, and varying atmospheres. There are three stages during coal formation: i) microbial, ii) biochemical, and iii) geochemical. During this alteration of organic material, impurities can become trapped in the coal. Some of these impurities include oxides, silicates, sulfides, sulfates, and chlorides. Sulfur can be present in coal in three different forms: (i) organic sulfur, which is chemically linked to the coal structure and difficult to remove with typical coal cleaning; (ii) sulfates which are soluble in water and easily removed; and (iii) pyritic sulfur which can be removed by physical cleaning, such as magnetic, gravity or screening methods. [10] The amount of sulfur in coal depends on:

1. Source region
2. Geologic history
3. Depth of coal in the seam

The interest of the present study is the removal of organic sulfur. As the coal burns, organic sulfur compounds are converted to H<sub>2</sub>S, COS (carbonyl compounds), and other sulfur species which can be removed with mixed metal oxide sorbents.

Table 1.1 lists some coals and their sulfur content from seams across the United States. [10] In order to utilize the high sulfur coals and comply with Federal regulations, the technology of using metal oxide sorbents for desulfurization needs to be improved.

### 1.3 Desulfurization Principles

The basic principle of sulfur removal (H<sub>2</sub>S and COS) from coal-combustion generated hot gas by mixed metal oxide sorbents can be expressed by the following reactions:

1.  $\text{MO}(\text{solid}) + \text{H}_2\text{S}(\text{vapor}) \rightarrow \text{MS} + \text{H}_2\text{O}$  (sulfidation)
2.  $\text{MS}(\text{solid}) + \text{O}_2(\text{vapor}) \rightarrow \text{MO} + \text{SO}_x$  (regeneration)

MO: single or mixed binary oxide

These reactions are solid-vapor and diffusion controlled. [7,8] The rate of reactions 1 and 2 are controlled by i) surface area, ii) pore volume, and iii) pore size distribution within the sorbents. [11,12] Depending on the prevailing conditions during sulfidation and regeneration (i.e., temperature, P<sub>O<sub>2</sub></sub>, and P<sub>H<sub>2</sub>O</sub>), other reactions are possible, such as the formation of sulfates. [13] Sulfate formation is undesirable because of the weakening and deterioration of the sorbent during sulfidation and especially during the regeneration cycle. [13,14] Sulfates also block the pores in the sorbent which

Table 1.1 Sulfur content in various coals from seams across the United States. [15]

Location of Mine	Coal Seam	% , Moisture Free Basis*			
		Total sulfur	Pyritic sulfur	Organic sulfur	Organic sulfur as percentage of total sulfur
Clearfield Co., PA	Upper Freeport	3.56	2.82	0.74	20.8
Allegheny Co., PA	Thick Freeport	0.92	0.46	0.45	48.9
Somerset Co., PA	C Prime	2.00	1.43	0.54	27.0
Franklin Co., IL	No. 6	2.52	1.50	1.02	40.5
Montgomery Co., IL	No. 6	4.97	2.53	2.40	48.3
Williamson Co., IL	No. 6	4.01	2.17	1.80	44.9
Union Co., KY	No. 9	3.28	1.05	2.23	68.0
Pike Co., KY	Freeburn	0.46	0.13	0.33	71.7
Boone Co., WV	Eagle	2.48	1.47	1.01	40.7
Letcher Co., WV	Elkhorn	0.68	0.13	0.51	75.0
Jefferson Co., AL	Pratt	1.72	0.97	0.72	50.0
Clay Co., IN	No. 3	3.92	2.13	1.79	45.7
Cumnock, NC	Deep River	2.32	1.52	0.8	34.5
Alleghany Co., MD	Big Vein	0.86	0.18	0.67	77.9
Meigs Co., OH	8-A	2.51	1.61	0.86	34.3

\*Sulfate sulfur is not recorded. The difference between the sum of the pyritic and organic sulfur and the total sulfur is sulfate sulfur.

prevents complete utilization of the sorbent and are not easily converted back to oxides.

[15]

A schematic diagram of the desulfurization process is shown in Figure 1.1. [16] In the simplest terms to describe the process, coal is burned with air and steam in the combustion chamber. The hot gas containing  $H_2S$  passes over a sorbent bed where the sulfur is removed and the cleaned air passes to the turbine or fuel cell to generate electricity. The sulfur trapped in the sorbent bed is eventually converted to sulfur dioxide during regeneration. The sulfur can be converted to elemental sulfur suitable for resale or converted into a disposable form, such as calcium or sodium sulfate. [2,5] To achieve high efficiency during the conversion process, the temperature of the gas leaving the combustion chamber should be as high as possible and the amount of steam added should be minimal. Having a sorbent bed that has a high sulfur intake capacity with high attrition resistance that can be used over many sulfidation/ regeneration cycles will reduce the cost of the process.

There are three types of configurations that can be used during the desulfurization process: fixed-bed, moving-bed, or fluidized bed. In a fixed-bed configuration, sorbent particles remain stationary throughout the sulfidation and regeneration process. Several reactor vessels operate simultaneously in either sulfidation or regeneration mode. Once a breakthrough concentration of  $H_2S$  in the exit gas is reached, the vessel's mode of operation is switched.

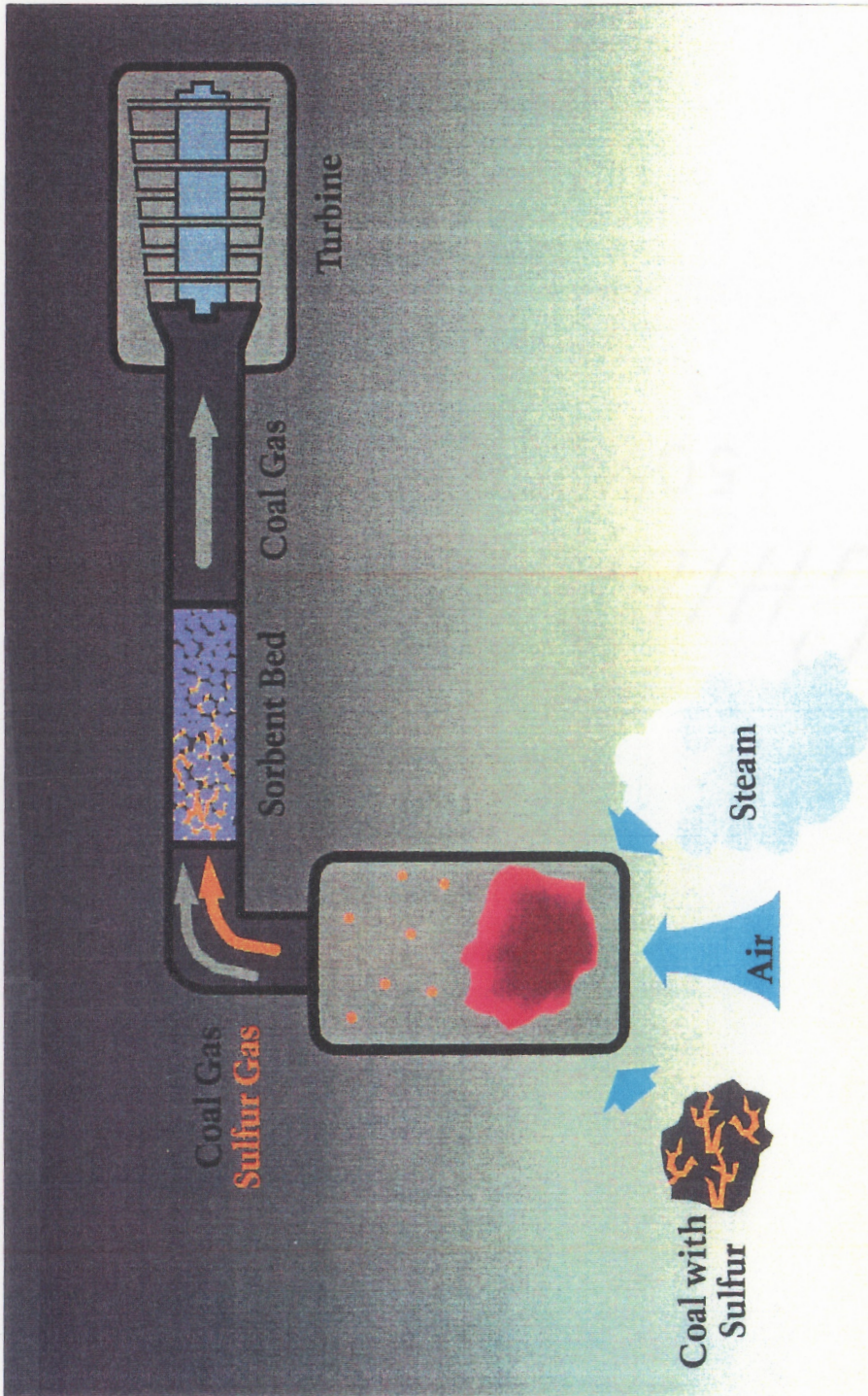


Figure 1.1 Schematic diagram of the desulfurization process. [16]

In a moving-bed system, the spent sorbent is removed from the bottom of the sulfidation vessel and fed to another for regeneration. The spent sorbent is replaced with fresh regenerated sorbent at the same time. Sorbent sulfur concentration and regeneration temperatures are easier to maintain using a moving-bed system. Sulfate formation is also minimized using this configuration. [9,17,18,19]

Fluidized-bed reactors offer operational advantages over the other reactors. Gas velocities in a fluidized-bed suspend the sorbent particles in a fluid-like state. The reactor operates at a uniform bed temperature and allows for a heat recovery system to be included in the temperature control design. [9] There is also good gas-solid contact which minimizes the diffusion distances and results in faster kinetics. [19] These fluidized-bed systems are being developed with high inlet temperatures of  $\sim 815^{\circ}\text{C}$ . [13]

Based on the principles for desulfurization and the demands of fixed-, moving-, and fluidized-bed reactors, sorbent pellets should meet the following criteria for efficient sulfur removal and long term use: [13,14,20]

- i. maintain high chemical reactivity (sulfur absorption and sulfur intake capacity)
- ii. maintain high mechanical strength, measured by the crush strength and attrition resistance
- iii. be capable of regeneration to an oxide at high temperatures without physical degradation of the pellet
- iv. maintain high porosity and surface area during successive sulfidation/regeneration cycling

## 1.4 Background of Sorbent Compositions

The practice of sulfur removal from hot coal-derived gases using metal oxide sorbents dates back to the first decade of the 19th century. [21] The U. S. Department of Energy/Morgantown Energy Technology Center (DOE/METC) has been involved in hot gas desulfurization projects for the past 15 years. Westmoreland et al. reported the results of a thermodynamic screening of the high-temperature desulfurization potential of 28 single-metal oxides using Gibbs free energy minimization method. [7,8] From this screening, initial investigations centered on single oxide sorbents ( $AO_x$ ) with iron and zinc oxides being the focus. However, due to physical degradation of the sorbents caused by loss of metallic iron vapor or zinc vapor through reduction of the oxides at low temperatures ( $\sim 500^\circ\text{C}$ ) and low efficiency of  $\text{H}_2\text{S}$  removal, the sorbent composition was later shifted to binary mixed metal oxides ( $ABO_x$ ). [22]

Various combinations of metal oxides were tried at the Massachusetts Institute of Technology (MIT) and the Jet Propulsion Laboratory (JPL) in an effort to design a durable and high capacity mixed metal oxide sorbent for sulfur removal. [23] The sorbents tested can be divided into two groups: 1) zinc-based, and 2) copper-based. Although copper-based sorbents have the potential to reduce sulfur levels to less than 1 ppm in the temperature range of  $538$  to  $732^\circ\text{C}$  [25], zinc-based sorbents were found to perform better than the copper-based sorbents because of the highly exothermic reduction of copper oxide by coal gas leading to temperature 'run-away' problems in sulfidation

reactors. [24] Zinc-based sorbents include zinc ferrite (ZF), zinc titanate (ZT), zinc-copper ferrite (ZCF), and zinc-copper aluminate (ZCA).

Initial studies on zinc-based sorbents centered on zinc ferrite,  $\text{ZnFe}_2\text{O}_4$ . However, under the typical oxygen partial pressure in coal gasification,  $10^{-20}$  atm or less, the stable phase of iron could be either  $\text{Fe}_3\text{O}_4$ ,  $\text{FeO}$ , or metallic iron. Under these conditions,  $\text{ZnFe}_2\text{O}_4$  is readily reduced to  $\text{Zn}^0$  or  $\text{ZnO}$  and  $\text{Fe}_3\text{O}_4$ ,  $\text{FeO}$ , or  $\text{Fe}^0$  resulting in loss of both iron and zinc by vaporization. [25] In order to prevent the formation of undesirable iron and zinc sulfates, special procedures need to be followed. [25] Therefore, zinc ferrite is limited to an operating temperature below  $550^\circ\text{C}$  and for coal gas containing at least 15% steam. [2,3,17] Increasing the amount of steam has several drawbacks. The heating value of steam is reduced therefore making the coal more difficult to burn. Additionally, as the volume of gas is increased with the increase in steam additions, the size of the system needed to handle the gas volume increases and thus the cost increases. [26]

Of the other zinc-based sorbents tested, zinc titanate,  $\text{Zn}_2\text{TiO}_4$ , has been found to have fewer limitations than  $\text{ZnFe}_2\text{O}_4$ .  $\text{Zn}_2\text{TiO}_4$  is stable to lower oxygen partial pressures than  $\text{ZnFe}_2\text{O}_4$ . [25] Therefore,  $\text{Zn}_2\text{TiO}_4$  can be used at higher operating temperatures ( $\sim 700^\circ\text{C}$ ) and under highly reducing coal gas containing less than 5% steam. [2]

Additions of  $\text{TiO}_2$  stabilizes  $\text{ZnO}$  against reduction to metallic  $\text{Zn}$  by reducing the amount of  $\text{Zn}^{2+}$  cations on the surface. [18,27,28] Vaporization of  $\text{Zn}$  at temperatures higher than  $699^\circ\text{C}$  has been reduced to about 1 wt%  $\text{Zn}$  is lost in 1000 hours of operation with additions of  $\text{TiO}_2$ . [4] Since  $\text{TiO}_2$  does not reduce under these conditions and titanium

does not react with  $H_2S$  and both Zn and Fe form sulfides, zinc titanate has a lower sulfur intake capacity and reacts slower with sulfur than zinc ferrite. [4,6,29] In order to minimize zinc vaporization and stabilize ZnO at elevated temperatures, there is a tradeoff in properties with the sulfur absorption lower using  $Zn_2TiO_4$ .

The sorbents described were tested as extruded pellets. An alternative approach was to distribute the sorbent powder on a passive ceramic support, such as zeolites. [24] The advantages of the supported sorbents are higher surface area, less resistance to diffusion-driven transport, and higher temperature and attrition resistance compared to bulk sorbents. Swisher applied this technique using Ni or  $Zn_2TiO_4$  as the sorbent on a ceramic support. In the latter case, excess  $TiO_2$  (33.33% ZnO and 66.67%  $TiO_2$  by weight) was used as a support resulting in an enhancement of compressive strength of the pellets. [30]

## 1.5 Zinc Titanate System

Extensive data regarding the sulfur uptake capacity and regenerability of the various sorbents are discussed in the literature. However, there is a lack of information concerning the crystal chemistry and characterization of the sorbents or the sulfidized phases based on x-ray diffraction analysis. The zinc-based compositions ZF, ZT, and ZCF should have a spinel or pseudospinel structure as the major phase of the sorbent. No explicit characterization is described in the literature. Lew et. al reported a multiphase assemblage of their zinc titanate based sorbent indicating incomplete reaction. [4] Also, a

review of the literature showed the Zn/Ti ratio has not been optimized for the zinc titanate sorbents. The published phase diagram of the system ZnO-TiO<sub>2</sub> shows only two stable phases, Zn<sub>2</sub>TiO<sub>4</sub> and ZnTiO<sub>3</sub>, with Zn/Ti atomic ratios of 2 and 1, respectively. [17,32] Another compound, Zn<sub>2</sub>Ti<sub>3</sub>O<sub>8</sub>, has been reported to form between 600 and 900°C. [32,33,34] However, subsequent reports showed that this is a metastable compound formed using the anatase form of TiO<sub>2</sub> or any organic precursor for Ti. With prolonged heating above 900°C, this compound converts to Zn<sub>2</sub>TiO<sub>4</sub> and TiO<sub>2</sub>, a recent report showed that the initial sorbent consisted of some Zn<sub>2</sub>Ti<sub>3</sub>O<sub>8</sub> which after several sulfidation and regeneration cycles was converted to Zn<sub>2</sub>TiO<sub>4</sub>. [13]

An optimized ratio between 1.5 and 2.0 was suggested based on the reaction kinetics and analysis of the phase assemblages formed. [13,35] In this range, Zn<sub>2</sub>TiO<sub>4</sub> is the principal phase, and there is no free ZnO. The presence of free ZnO cannot be tolerated because it can initiate zinc vaporization. [13]

As discussed in Section 1.3, desulfurization is a solid-vapor reaction and diffusion controlled. [7,8] Diffusion reactions are very sensitive to the structure and physical properties of the solid phases involved. Knowledge of these phases is important when studying the kinetics and extent of the desulfurization process and correlating with pore volume, particles size, and other properties of the sorbent phase. [17,32]

Although zinc titanate (Zn<sub>2</sub>TiO<sub>4</sub>) based sorbents showed the most promise, several problems still exist which limit its efficiency in sulfur removal and durability over many sulfidation/regeneration cycles. These problems include:

- 1) **temperature limitation for sulfidation**
- 2) **zinc loss**
- 3) **low attrition resistance**
- 4) **physical degradation**

## 2.0 OBJECTIVES AND APPROACH

The ultimate goal of this research is to improve the sulfidation and regeneration performance of zinc titanate sorbents. In the present study, the approach to eliminate the problems with zinc titanate is to modify the composition of the  $Zn_2TiO_4$  spinel phase by incorporating cations into the  $Zn_2TiO_4$  lattice. By utilizing the principles of solid-state science, including phase equilibria, crystal chemistry, and thermochemistry, appropriate ions can be selected and incorporated to determine the effectiveness in sulfur removal. Most sorbent compositions were developed essentially on the basis of the sulfur uptake ability of the metal oxides. An in-depth investigation was not done of the phase equilibria, crystal chemistry, and the mutual interactions between the phases present in the sorbent. The current approach will help provide an understanding of the physical and chemical behavior of the sorbent during processing, sulfidation, and regeneration.

### 2.1 Objectives

The purpose of this study is to investigate any changes in the desulfurization performance of the zinc titanate sorbent as a function of cationic substitutions. The focus and specific objectives of this research include the following:

1. Select cations for substitution in the  $Zn_2TiO_4$  spinel lattice.
2. Determine the range of solid-solubility of the selected cations in the  $Zn_2TiO_4$  spinel lattice.
3. Determine and understand the effects of the type and concentration of substituted cations on the fresh, sulfidized and regenerated sorbent (including attrition, particle size, and porosity).

The solubility or extent of incorporation of the cations is measured through the lattice parameter change of the  $Zn_2TiO_4$  spinel phase. Ionic substitutions and lattice parameter changes in many spinel phases have been studied and reported; however, substitutions in the  $Zn_2TiO_4$  lattice have not been reported. [36] Once the physical and chemical properties of the sorbent during all stages of the desulfurization process have been determined,  $Zn_2TiO_4$  sorbents can be designed to meet the needs of more challenging desulfurization conditions.

## 2.2 Crystal Chemistry of Spinel

In order to select appropriate ions to be incorporated into the  $Zn_2TiO_4$  lattice, the spinel structure is reviewed. The mineral spinel ( $MgAl_2O_4$ ) has given its name to a large class of compounds having the same crystal structure. A spinel has the general formula  $AB_2O_4$  or  $A_8B_{16}O_{32}$  per unit cell. The spinel structure consists of 32 oxygen anions

arranged in a cubic close-packed structure. This arrangement leaves 64 tetrahedral and 32 octahedral holes as possible sites for cations, of which only 8 tetrahedral (A) and 16 octahedral (B) positions are occupied as illustrated in Figure 2.1. [37] The 24 cations and 32 oxygen ions constitute a face-centered cubic cell with a unit cell edge of approximately 8 angstroms (Å) depending on the composition and distribution of cations in the four- and six-fold coordinated positions. [38,39]

In the formula unit ( $AB_2O_4$ ) of spinels, there are three cations with a total valency of eight. The electrostatic balance can be satisfied by various combinations of cations of different charges; however, the geometrical conditions limit the radii of these cations within the range of 0.44Å to 1.0Å with the exception of  $Ag^+$  ( $r = 1.29\text{Å}$ ). [38] Cation and anion vacancies have also been reported. [40]

The following possible variations in cation arrangement in spinels was suggested by Barth and Posnjak from x-ray diffraction studies. [41]

- i. 'Normal' spinel with similar cations occupying similar coordinating positions:  $A^{IV}B_2^{VI}O_4$ .
- ii. 'Inverse' spinel with similar cations occupying different coordinating positions:  $B^{IV}(AB)^{VI}O_4$ .
- iii. 'Random' spinel:  $(A_{1-x}B_x)^{IV}(A_xB_{2-x})^{VI}O_4$ .

The ionic distribution in the  $Zn_2TiO_4$  structure can be represented by  $(Zn)^{IV}(ZnTi)^{VI}O_4$ .

[39] Table 2.1 provides a set of relative site preference energies to predict the probable ionic distribution in spinels. [38,40,42] In this table, the higher the energy, the greater the

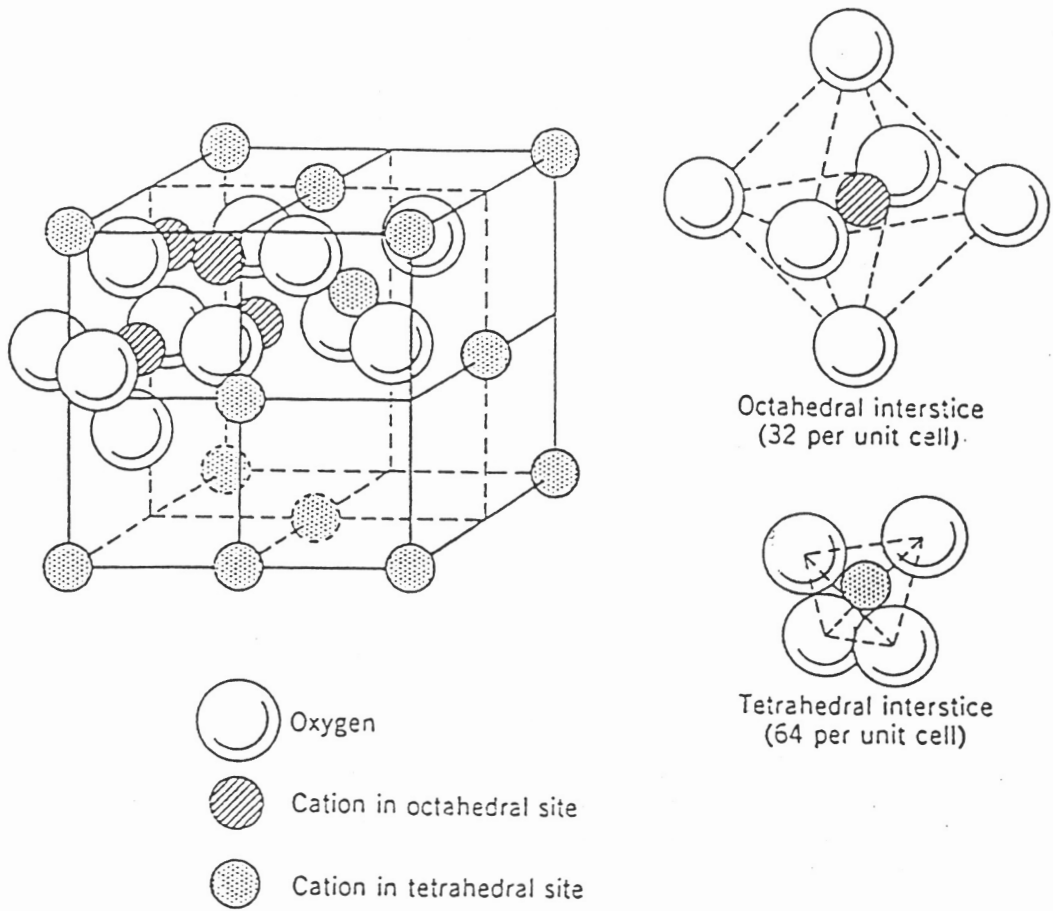


Figure 2.1 Spinel structure. [37]

Table 2.1 Site preference energies for various cations in spinels.\* [43]

Ion	P		Ion	P		Ion	P
Mg <sup>2+</sup>	-5.0		Co <sup>2+</sup>	-10.5		Mn <sup>2+</sup>	-14.7
Al <sup>3+</sup>	-2.5		Zn <sup>2+</sup>	-31.6		Fe <sup>3+</sup>	-13.3
Ni <sup>2+</sup>	9.0		Ca <sup>2+</sup>	-30.7		Cr <sup>3+</sup>	16.6
Fe <sup>2+</sup>	-9.9		Ti <sup>3+</sup>	-21.9		Cu <sup>2+</sup>	-0.1

\*Values of P are in K cal/g-atomic weight. The larger and more positive the values of P, the greater is the preference of the ion for the octahedral site in the spinel structure.

probability of the ion to occupy an octahedral site. For example, Cr, Ti, and Ni are more likely to occupy octahedral sites, whereas Zn, Al, and Cu are more likely to occupy the tetrahedral site. Numerous cations of bi-, tri-, or higher valencies can be introduced in the spinel lattice. Only those cations which have the potential for improving the sulfidation and regeneration properties of the sorbent will be used in the substitutions.

### 2.3 Cation Selection

For the present study, only a few cations were selected based on the following guidelines for improvement of zinc titanate sorbent performance:

1. ionic size and charge
2. possible reduction in associated volume change during sulfidation to improve attrition resistance
3. improved sulfidation capability and easy regeneration
4. improved attrition resistance through introduction of refractory oxides
5. stability of oxides under different temperature and reducing conditions

Based on these guidelines, the following cations were selected for substitution in the  $Zn_2TiO_4$  lattice:  $Ni^{2+}$ ,  $Cr^{3+}$ ,  $Al^{3+}$ ,  $Mg^{3+}$ , and  $Cu^{2+}$ . The rationale behind the selection of these cations and the approach based on atomic substitutions to improve the sorbent's sulfidation performance can be described in a few examples.

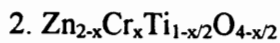


Table 2.2 Ionic radii for ions used in this study. [41]

Ion	Radius (Å)
Zn <sup>2+</sup>	0.83
Ti <sup>4+</sup>	0.69
O <sup>2-</sup>	1.32
Ni <sup>2+</sup>	0.78
Mg <sup>2+</sup>	0.78
Cu <sup>2+</sup>	0.8
Cr <sup>3+</sup>	0.64
Al <sup>3+</sup>	0.57

change observed in reaction 2. [44] It is known that a significant amount of Ni can be introduced in the  $Zn_2TiO_4$  lattice to form  $Zn(Zn_{1-x}Ni_xTi)O_4$ . [36]

**3. Sulfur Uptake:** Since Ti does not form a sulfide during desulfurization, only about 35-45% of the  $Zn_2TiO_4$  weight is utilized in sulfur removal. Maintaining the spinel structure while replacing some Ti with a sulfide forming ion, such as  $Cr^{3+}$ , would improve the efficiency of the sorbent. The theoretical sulfur capacity for  $Zn_2TiO_4$  is 26.4 g S/100 g sorbent. [2] Addition of as little as 6 mole percent Cr could improve the sulfur capacity by at least 10%. Figure 2.2 shows the theoretical weight gain for completely sulfided  $Zn_2TiO_4$  as a function of Cr incorporation. As expected with increasing additions of Cr, the sulfur intake capacity increases as more Ti is replaced by the sulfide forming Cr ion. Maintaining the charge balance,  $Cr^{3+}$  can be introduced into the  $Zn_2TiO_4$  lattice in three ways:



In addition, substitution of any  $Zn^{2+}$  ion by  $Cr^{3+}$  ion could cause 50% more sulfur removal ( $ZnS$  vs.  $CrS_{1.5}$ ).

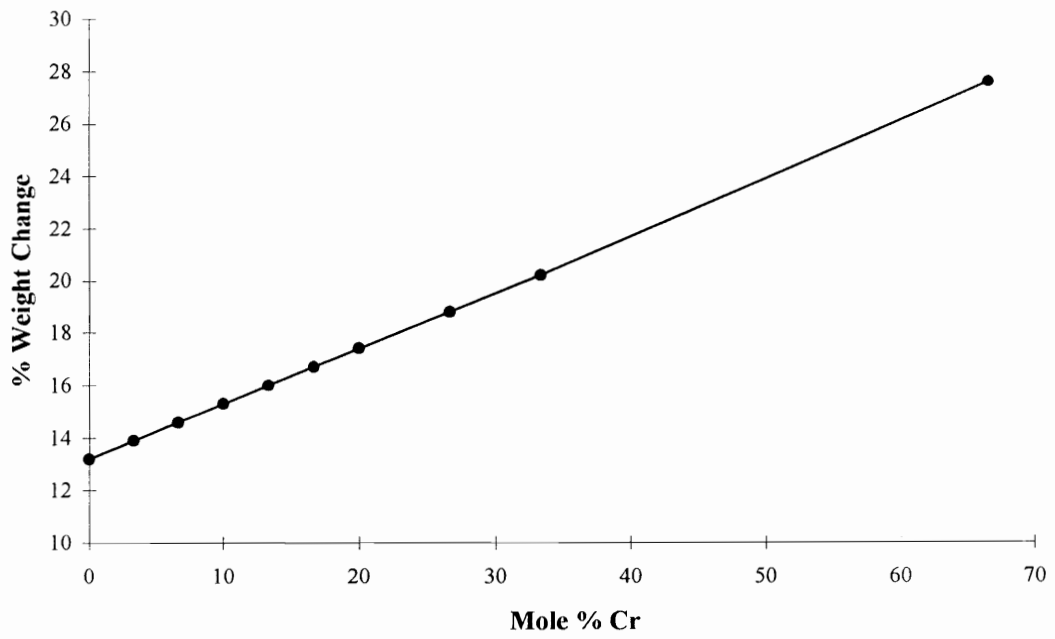


Figure 2.2. Theoretical weight gain of completely sulfidized  $Zn_2TiO_4$  with increasing additions of Cr.

**4. High-temperature operability and improved attrition resistance:**  $\text{Al}_2\text{O}_3$ ,  $\text{MgO}$ , and  $\text{Cr}_2\text{O}_3$  are well known refractory oxides. Introducing these ions in the  $\text{Zn}_2\text{TiO}_4$  lattice can enhance the sinterability and help reduce the zinc loss of the sorbent by providing a support for the  $\text{Zn}_2\text{TiO}_4$  phase. Incorporation of these ions can also improve its recyclability and operability at higher temperature.  $\text{Al}^{3+}$  and  $\text{Mg}^{2+}$  ions do not participate in the sulfidation reaction [45], so there is a tradeoff in obtaining mechanical strength but reducing the sulfur uptake ability. Mg can be incorporated using the general formula  $\text{Zn}(\text{Zn}_{1-x}\text{Mg}_x\text{Ti})\text{O}_4$  and Al using the formula  $\text{Zn}(\text{Zn}_{1-x}\text{Al}_{2x}\text{Ti}_{1-x})\text{O}_4$ .

**5. Stability of oxides under reducing conditions of coal combustion:** Typical conditions during gasification are temperatures between  $500^\circ\text{C}$  and  $800^\circ\text{C}$  and oxygen partial pressures of  $10^{-20}$  atm or less.  $\text{Cr}_2\text{O}_3$ ,  $\text{Al}_2\text{O}_3$ , and  $\text{MgO}$  are more stable under the gasification conditions than  $\text{ZnO}$ . [46] Additions of the various cations could help stabilize  $\text{ZnO}$  so reduction to and subsequent vaporization of metallic Zn would be minimized.

## **3.0 EXPERIMENTAL PROCEDURE**

The purpose of this research is to investigate any change in the desulfurization performance of the sorbents as a function of cationic substitution. There are several sections to this study:

1. solid-solubility determination
2. characterization of the pellets including density, porosity, and crush strength
3. sulfidation/regeneration performance

The first part is to establish the solubility range for each cation, once the extent of cationic incorporation is determined, pellets can be prepared and characterized to study any effects of the incorporated cations on the sulfidation/regeneration properties of the sorbent.

### **3.1 Sample Preparation**

#### **3.1.1 Powder Synthesis**

To determine the extent of solubility of the cations in the zinc titanate spinel lattice, reagent-grade oxides (ZnO, TiO<sub>2</sub>, Cr<sub>2</sub>O<sub>3</sub>, Al<sub>2</sub>O<sub>3</sub>, NiO, MgO, and CuO) were used as starting materials, see Appendix A. Appropriate proportions were weighed on a Sartorius balance (Model 1872) to an accuracy of +/- 0.1 mg. Each formulation was mixed under acetone in a glass mortar with pestle and allowed to air dry at room temperature. The process of mixing and drying was repeated three to four times. One

gram from each of the formulations was fired in a programmable Thermolyne (No. 1500) furnace in an open alumina crucible. All samples were fired for 24 hours in air at temperatures of 900, 1000, and 1100°C.

### 3.1.2 Pellet Preparation

Based on the solubility data and preliminary screening of all systems by Southern Illinois University at Carbondale (SIUC), the  $Zn_2TiO_4 - Cr_2O_3$  system showed the most promise, in terms of chemical reactivity and stability, and was selected for further testing. [47] Appropriate proportions of reagent-grade oxide powders were mixed in a glass mortar with pestle for approximately 30 minutes. A binder solution was prepared by dissolving 10 grams of reagent-grade starch in 300 ml of distilled water and heating to the boiling point when a clear solution was obtained. The oxide mixture was blended with the starch solution until the material had a consistency of toothpaste. It was then extruded through a 1 cm diameter metal tube and cut to lengths of approximately 1.5 cm. After drying at  $\sim 70^\circ C$  overnight, the green pellets were sintered for 3 hours at 900 - 1000°C in a Thermolyne furnace (No. 1500).

#### 3.1.2.1 Larger Particle Size ZnO and $TiO_2$

In order to improve the porosity of  $Zn_2TiO_4$ , larger particle size precursor oxides were procured. ZnO was prepared by roasting ZnS (mean particle size of 10 $\mu m$ ) in air for at least 6 hours at 850°C.  $TiO_2$  with a mean particle size of 2  $\mu m$  was procured from Alfa

Aesar Products. Pellets using these powders were prepared using the same method described in the previous section.

## **3.2 Characterization**

### **3.2.1 X-ray Diffraction Analysis**

X-ray diffraction patterns were obtained for identification of crystalline phases and calculation of lattice parameter values for both the powders and sorbent pellets, before and after sulfidation and regeneration testing. A Philips PW1729 X-ray diffractometer employing CuK $\alpha$  radiation and operating at 40 kV, 30 mA was used for all analysis. A scanning rate of 3°-2 $\Theta$ /min was used for phase identification and rate of 1.5°-2 $\Theta$ /min for lattice parameter measurements. All x-ray measurements were made at room temperature.

### **3.2.2 Density and Porosity Measurements**

Theoretical and bulk densities of the sintered pellets were determined for each composition. The theoretical density ( $\rho$ ) was calculated using the lattice parameter values obtained from XRD, a sample calculation is included in Appendix C. The bulk density ( $\rho_o$ ) was measured using a hydrostatic method (ASTM C 373-88) where the pellets were weighed dry, suspended in water, and after saturation in water for 24 hours. The porosity of the pellets was calculated as the difference between these values using the formula:

$$\% \text{ Porosity} = 100 \times ((\rho - \rho_o)/(\rho))$$

A Horiba LA700 Laser Scattering Particle Size Distribution Analyzer with an accuracy of +/- 10% was used to determine the particle size distribution and mean particle size of the precursor oxides and sintered materials.

### **3.2.3 Stability of Cr-Incorporated Sorbents**

To determine the stability and to detect any exsolution of the solid-solution phases at 650°C (the temperature selected for testing of sorbents), six compositions previously equilibrated to 1100°C and characterized by x-ray diffraction as a single phase of spinel solid-solution were heated at 650°C and held for 1.5, 3, and 5 days. X-ray diffraction patterns were obtained on all samples and lattice parameters measured.

### **3.2.4 Crush Strength Measurements**

At SIUC, crush strength measurements were made in a Material Test System (MTS-810) apparatus equipped with an Intertaken DDC 4000 Controller at a loading rate of 0.0254 cm/min. ASTM test procedures for compression testing of ceramic materials and catalyst particles was used. The cylindrical pellets were held in a plunger-type specimen holder designed and fabricated for the project. Prior to testing, both ends of the pellets were ground flat with emery papers to minimize premature failure due to buckling. Crush strength was obtained by subjecting each pellet to an increasing load until failure. Six to ten specimens were tested for each composition and an average calculated.

### **3.2.5 Thermogravimetric Analysis (TGA)**

#### *3.2.5.1 Testing at Southern Illinois University (SIUC)*

At SIUC, the sintered pellets were tested in a DuPont-951 Thermogravimetric Analyzer (TGA) to study the reactivities of the different sorbents. The TGA is equipped with an Innovative Thermal Systems component and software, which controls the operating temperature and times, and an Atari 520ST™ computer, which stores and manipulates acquired data. The reactivity of different sorbent materials was determined by measuring weight changes of single, small pieces (40 to 70 mg) of the sintered sorbent as a function of time during sulfidation in 1% H<sub>2</sub>S in H<sub>2</sub> or simulated coal gas, listed in Table 3.1, and regeneration in air or diluted air. The experiments were conducted at atmospheric pressure and 650°C for two sulfidation-regeneration cycles.

The weight of each sample was also measured with a Sartorius Balance (Model A120S) before and after the TGA test. These measurements were used to check and correct TGA results in case of instrument zero point shifting and carbon deposition onto the sample basket and suspending rod when simulated coal gas was used. Nitrogen was used to purge the reactor chamber during heating and was replaced with reactant gas when the temperature reached the set point. When the reaction was complete, nitrogen was used again to purge the chamber during cooling.

Table 3.1 Composition of simulated coal gas used in TGA tests at SIUC.

Component	Starting Composition	Equilibrium Composition (650°C)
H <sub>2</sub>	49.5%	33.8%
H <sub>2</sub> O	1.0%	14.4%
CO	17.0%	26.0%
CO <sub>2</sub>	32.0%	22.7%
CH <sub>4</sub>	-----	2.6%
H <sub>2</sub> S	0.5%	0.5%
O <sub>2</sub>	-----	1x10 <sup>-23</sup>
S <sub>2</sub>	-----	2x10 <sup>-9</sup>

### **3.2.5.2 Testing at Research Triangle Institute (RTI)**

Thermogravimetric Analysis (TGA) was performed on samples with and without Cr to study the effect of Cr additions on Zn losses due to vaporization during sulfidation. Pellets prepared by the method described in Section 3.1.2 were sent to Research Triangle Institute for testing. The procedure used consisted of the following steps:

1. Heat the sample up to the desired temperature (750°C) with a purge.
2. 15-min reduction at 750°C in an H<sub>2</sub>S-free clean coal gas.
3. 30-min sulfidation at 750°C in a simulated coal gas.
4. Hold at 750°C after sulfidation in the simulated coal gas. No additional gases are allowed into the analyzer.

The gases used during the experiments are listed in Table 3.2. For a more detailed description of the test procedure refer to reports by R. Gupta. [13]

### **3.2.6 EDX Analysis**

Semi-quantitative chemical analysis was performed on the Cr-incorporated samples after sulfidation using an Electroscan Environmental Scanning Electron Microscope with an Energy Dispersive X-ray (EDX) analysis system. This testing was used to determine the amount of Zn present on the surface of the sorbent after sulfidation testing.

Table 3.2. Composition of the gases used in TGA tests at RTI.

Component	Volume Percent	
	Reduction <sup>a</sup>	Sulfidation <sup>a</sup>
CO <sub>2</sub>	11.90	11.21
CO	37.45	37.88
H <sub>2</sub>	30.75	29.80
N <sub>2</sub>	-----	-----
H <sub>2</sub> O	19.90	19.90
O <sub>2</sub>	-----	-----
H <sub>2</sub> S	-----	1.21

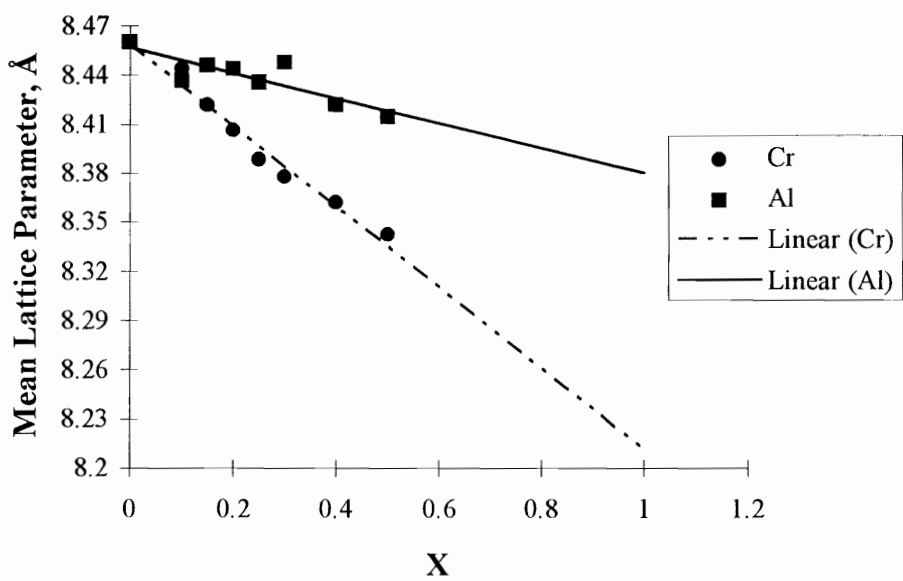
<sup>a</sup>Simulated Texaco-type medium BTU gas.

## 4.0 EXPERIMENTAL RESULTS AND DISCUSSION

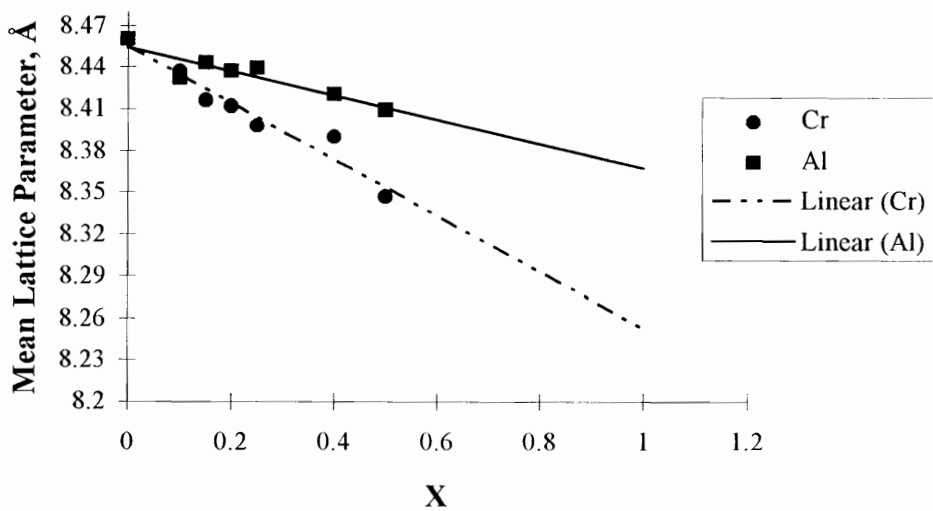
### 4.1 Solubility Range Determination for All Selected Cations

The extent of equilibrium cation incorporation in the  $Zn_2TiO_4$  lattice between 900 and 1100°C was determined for the systems  $Zn_2TiO_4 - MO_x$ , where  $M = Ni, Cr, Al, Mg,$  and  $Cu$ . The approach involved phase purity checks of the equilibrated samples and lattice parameter measurements of the resulting spinel phases by XRD. Since the interest was in the relative change in lattice parameter,  $a_0$ , no internal standard was used; however, the equipment is routinely calibrated. The (511) and (440) reflections were used in calculating the lattice parameter of the spinel phases. For all systems, a decrease in lattice parameter,  $a_0$ , with an increase in substitutional cation concentration is observed indicating incorporation of the cations into the  $Zn_2TiO_4$  lattice. The ionic radii of all cations is smaller than  $Zn^{2+}$  and radii of  $Cr^{3+}$  and  $Al^{3+}$  are smaller than  $Ti^{4+}$  also. Figures 4.1 and 4.2 show the change in lattice parameter with increasing cation concentration for the five cations at 1000°C and 1100°C. For Ni, Mg, and Cu, the slope is gradual and increases as the difference between the radii of Zn and the cation becomes larger. The decrease becomes sharper for Cr and Al which can replace either Zn or Ti in the spinel structure. Although Al has a smaller radius than Cr, Al can be incorporated with less distortion to the lattice and therefore has a less steep slope than Cr.

XRD showed a single spinel solid-solution phase for compositions up to ~35 mole percent for  $Ni^{2+}$  ( $x = 0.7$ ),  $Cr^{3+}$  ( $x = 0.5$ ), and  $Al^{3+}$  ( $x = 0.5$ ) and up to ~25 mole percent

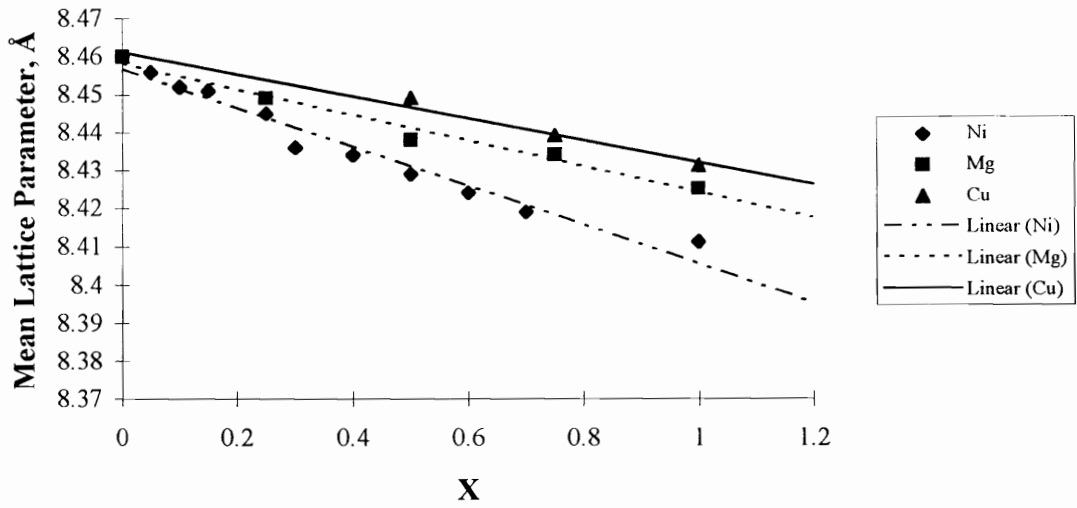


a)

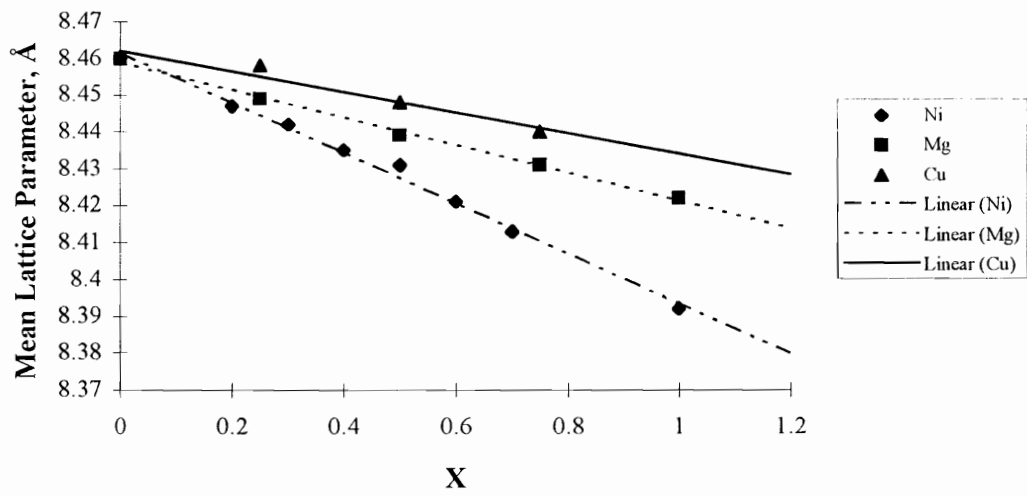


b)

Figure 4.1. Change in mean lattice parameter of the spinel phase for  $Zn_{2-x}Ti_{1-x}M_{2x}O_4$ ,  $M = Cr$  or  $Al$  at a) 1000°C and b) 1100°C.



a)



b)

Figure 4.2. Change in mean lattice parameter of the spinel phase for Zn<sub>2-x</sub>M<sub>x</sub>TiO<sub>4</sub>, M = Ni, Mg, or Cu at a) 1000°C and b) 1100°C.

for  $\text{Mg}^{2+}$  ( $x = 0.5$ ) at 1000 and 1100°C. This level is a saturation point for the cations in the  $\text{Zn}_2\text{TiO}_4$  lattice at 1100°C. Above this concentration, unreacted oxide phases appear in the XRD patterns and the percentage increases with higher concentrations of cations. At 900°C, the spinel solid-solution phase is present along with unreacted oxides indicating incomplete reaction. The starting compositions, firing temperature, and phases present for the five systems are listed in Appendix B. The spinel solid solution phase is denoted by either  $(\text{ZnM})_2\text{TiO}_4$  for  $M = \text{Ni}, \text{Mg}, \text{and Cu}$  or  $(\text{ZnTiM})_3\text{O}_4$  for  $M = \text{Cr and Al}$ .

The saturation limit could not be determined for Cu fired in alumina crucibles due to low-temperature melting and emergence of a liquid phase resulting in severe sintering above 1000°C. However, at least 12.5 mole percent Cu could be incorporated before the sintering becomes severe. When the experiments were repeated using platinum, the saturation level was determined to be ~37 mole percent ( $x = 0.75$ ) at 1000 and 1100°C.

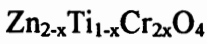
## 4.2 ZnO - TiO<sub>2</sub> - Cr<sub>2</sub>O<sub>3</sub> System

The ZnO - TiO<sub>2</sub> - Cr<sub>2</sub>O<sub>3</sub> system was chosen for further study based on the solubility measurements and preliminary screening using TGA testing at SIUC. [47] Cr-incorporated samples had better sulfur removal capacity and reactivity over the other cations studied. The focus of the study was then to determine the effects of cation substitution mode and concentration on the performance of the sorbent for fixed bed tests.

#### 4.2.1 Mode of Substitution

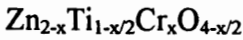
In the system ZnO - Cr<sub>2</sub>O<sub>3</sub> - TiO<sub>2</sub>, solid solutions in the spinel phase, Zn<sub>2</sub>TiO<sub>4</sub>, can take place in three different ways, shown as the joins between Zn<sub>2</sub>TiO<sub>4</sub> and 1) ZnCr<sub>2</sub>O<sub>4</sub>, 2) Cr<sub>2</sub>O<sub>3</sub>, and 3) Cr<sub>2</sub>TiO<sub>5</sub> in Figure 4.3. The probable cationic arrangement for the three modes of substitution is described below:

Join 1. Zn<sub>2</sub>TiO<sub>4</sub> - ZnCr<sub>2</sub>O<sub>4</sub> Stoichiometric substitution



cationic arrangement:  $\text{Zn}^{\text{IV}}(\text{Zn}_{1-x}\text{Ti}_{1-x}\text{Cr}_{2x})^{\text{VI}}\text{O}_4$

Join 2. Zn<sub>2</sub>TiO<sub>4</sub> - Cr<sub>2</sub>O<sub>3</sub> Nonstoichiometric substitution - cation and anion vacancy



cationic arrangement:  $\text{Zn}^{\text{IV}}(\text{Zn}_{1-x}\text{Ti}_{1-x/2}\text{Cr}_x\text{O}_{x/2})^{\text{VI}}\text{O}_{4-x/2}$

Join 3. Zn<sub>2</sub>TiO<sub>4</sub> - Cr<sub>2</sub>TiO<sub>5</sub> Nonstoichiometric substitution - oxygen interstitial



cationic arrangement:  $\text{Zn}^{\text{IV}}(\text{Zn}_{1-2x}\text{TiCr}_{2x})^{\text{VI}}\text{O}_{4+x}$

In addition, various combinations of these three substitution types are possible, the shaded area of Figure 4.3. The cationic arrangements suggested above are based on the assumption that Zn<sup>2+</sup> can occupy both the IV and VI coordination positions but prefers the IV coordination position. Also, Ti<sup>4+</sup> and Cr<sup>3+</sup> occupy only the VI coordination position, see Table 2.1. [43] Each system obviously has an upper limit of x, beyond which further substitution will not be possible due to limitations imposed by the crystal chemistry or site preference of the substituting cations.

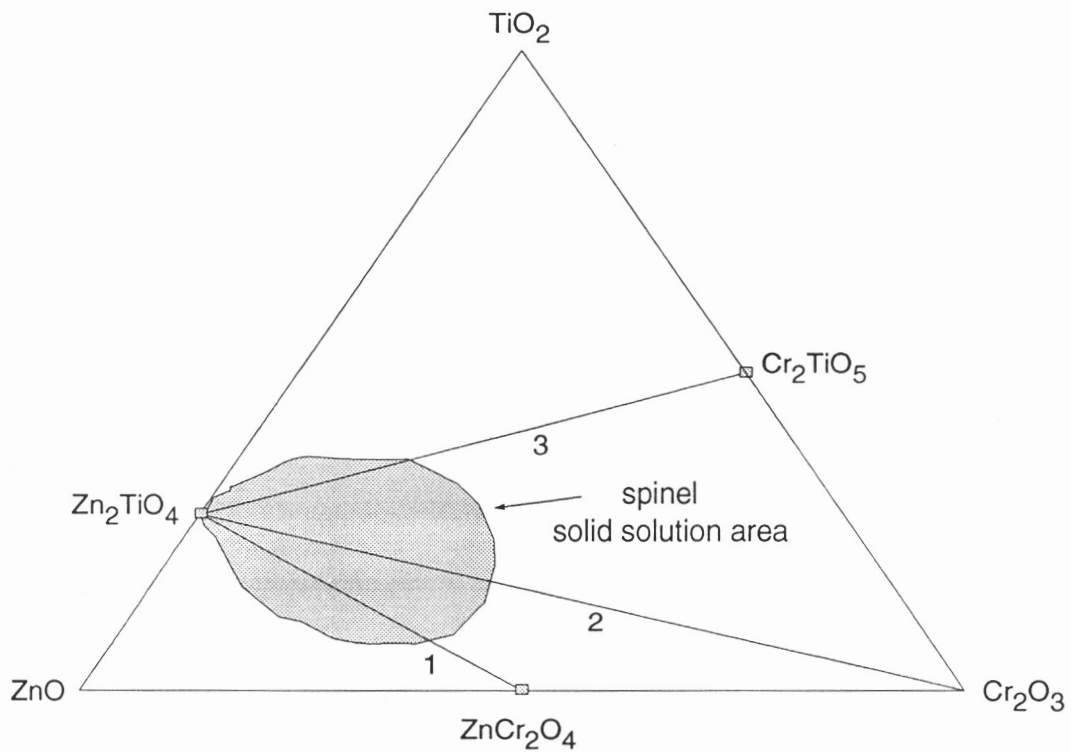


Figure 4.3 Phase diagram for the ZnO - TiO<sub>2</sub> - Cr<sub>2</sub>O<sub>3</sub> system showing the modes of substitution.

Changes in the lattice parameter of the phases forming a solid-solution series as a function of the concentration of the substituted ion depend on:

1. Size, charge, and electronic arrangement of the substituting ion: its polarizability
2. Nature of the substitution (stoichiometric, interstitial, or vacancy)
3. Coordination number of the substituting ion
4. Any rearrangement of the cationic coordination number due to the substitution
5. Temperature of equilibration (substitution)
6. Lattice type of the host crystal

Accordingly, the slope of the lattice parameter versus the amount of Cr substituted in these modes would be different. Therefore, different slopes would indicate different modes of substitution. In Figure 4.4, there is a definite trend in the slope of the lattice parameter decrease indicating the method of substitution. According to Flytzani-Stephanopoulos et. al, there are different sulfur absorption centers in the  $Zn_2TiO_4$  lattice. [18] It is possible that these different modes of substitution would change the nature of the absorption centers causing changes in the sulfur removal capacity of the different sorbents. These differences, if any, would be seen in the TGA results.

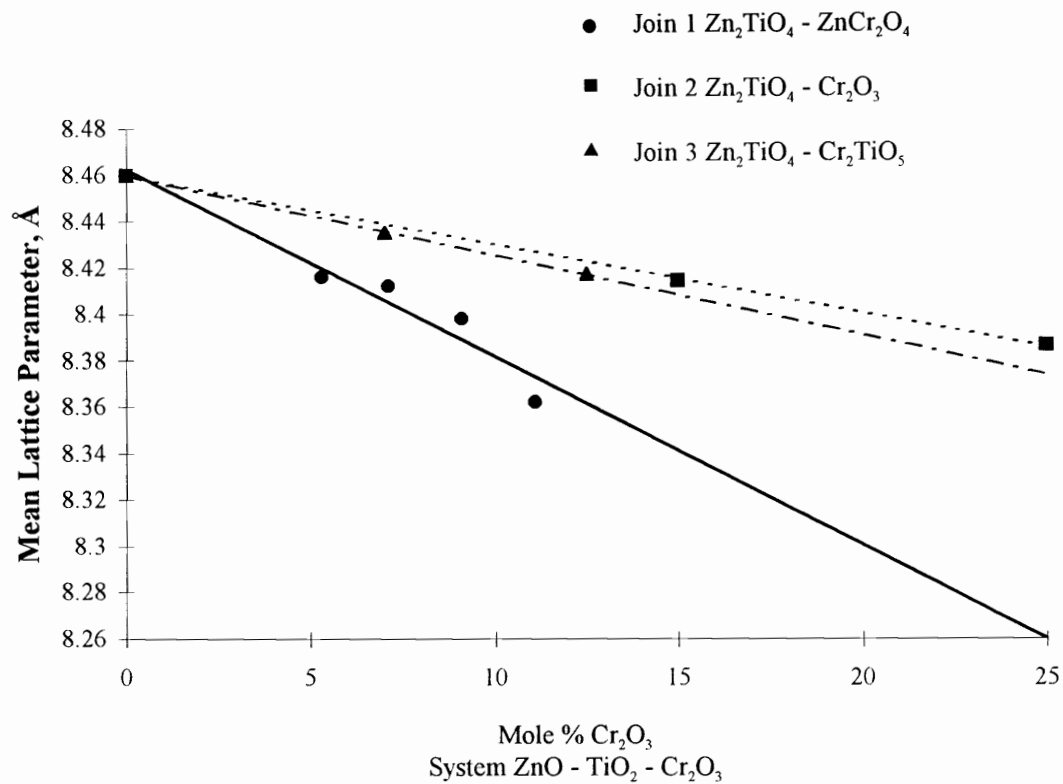


Figure 4.4. Trends in the change in mean lattice parameter of the  $Zn_2TiO_4$  phase with mode of Cr substitution.

## **4.3 Characterization of Cr-Incorporated Sorbents**

### **4.3.1 Stability of Sorbent at Sulfidation Temperatures**

All Cr-incorporated specimens were observed to form spinel solid solutions at 900-1100°C. However, it is not known if they might be stable or exsolve into two phases at 650°C, the temperature chosen for TGA and fixed bed testing. The stability was determined by calculating the lattice parameter of the specimens before and after prolonged treatments at 650°C and by identifying the phases present from XRD. Table 4.1 shows the results of lattice parameter measurements before and after prolonged treatment at 650. No changes in lattice parameter occurred even after heating for 5 days. Also, no additional phase was detected in the x-ray diffraction patterns which could be a decomposition product of the spinel phases.

### **4.3.2 XRD**

XRD was used to characterize the samples before they were submitted for TGA testing. At all three sintering temperatures, samples were identified as having a spinel solid-solution phase with trace amounts, less than 5 percent by weight, of oxides (ZnO or TiO<sub>2</sub>). Lattice parameter values were determined from the x-ray patterns for all samples at the respective sintering temperatures and used in the calculation of theoretical densities.

Table 4.1 Lattice parameter data for  $Zn_{2-x}Ti_{1-x}Cr_{2x}O_4$  prepared at 1100°C and held for various times at 650°C.

x	Average $a_o \pm 0.003 \text{ \AA}$			
	1100°C <sup>a</sup>	R1 <sup>b</sup>	R2 <sup>c</sup>	R3 <sup>d</sup>
0.10	8.437	8.436	8.433	8.437
0.20	8.412	8.413	8.411	8.412
0.25	9.398	8.397	8.397	-----
0.30	8.363	8.363	8.366	8.366
0.40	8.390	8.386	-----	8.387
0.50	8.347	9.347	8.349	8.346

<sup>a</sup>1100°C = prereacted for 24 hours

<sup>b</sup>1100°C and heated to 650°C for 1.5 days

<sup>c</sup>1100°C and heated to 650°C for 3 days

<sup>d</sup>1100°C and heated to 650°C for 5 days

### 4.3.3 Density, Porosity, and Crush Strength Measurements

Table 4.2 lists the densities and porosity for the compositions prepared in the ZnO-TiO<sub>2</sub> - Cr<sub>2</sub>O<sub>3</sub> system. The theoretical density was calculated on the assumption Cr is incorporated completely within the spinel structure, a sample calculation is shown in Appendix C. The sintering temperature was varied between 900 and 1000°C to determine the effect on the porosity. As expected the porosity decreases with increasing sintering temperature. Crush strength was also determined for all compositions, see Table 4.3. With increasing porosity, the crush strength decreases as would be expected. Depending on the properties which are more important during sulfur removal, high strength or high surface area, the sintering temperature can be varied to give the desired properties.

### 4.3.4 TGA Testing at SIUC

Thermogravimetric analysis (TGA) was performed on all compositions. The samples were tested in either a mixture of 0.9% H<sub>2</sub>S, 92.4% H<sub>2</sub>, and 6.7% N<sub>2</sub> or in simulated coal gas, listed in Table 3.1. Figures 4.5-4.8 are typical sulfidation and regeneration cycles for the various compositions tested in either the H<sub>2</sub>S gas mixture or simulated coal gas. The initial weight loss observed is attributed to loss of moisture. For the compositions tested in the H<sub>2</sub>S gas mixture, the weight gain is much higher. All samples were identified by XRD before TGA to be essentially a spinel solid-solution phase with trace amounts of ZnO and TiO<sub>2</sub> (less than 5 percent by weight).

Table 4.2 Density and porosity data for the Cr-incorporated sorbents.

Join	Composition	Sintering <sup>a</sup> Temperature, °C	Theoretical Density (g/cm <sup>3</sup> )	Bulk Density (g/cm <sup>3</sup> )	Porosity (%)
1	Zn <sub>1.9</sub> Ti <sub>0.9</sub> Cr <sub>0.2</sub> O <sub>4</sub>	900	5.35	2.62	51.9±3.6
1	Zn <sub>1.9</sub> Ti <sub>0.9</sub> Cr <sub>0.2</sub> O <sub>4</sub>	950	5.35	2.68	49.9±3.5
1	Zn <sub>1.9</sub> Ti <sub>0.9</sub> Cr <sub>0.2</sub> O <sub>4</sub>	1000	5.35	2.93	45.3±3.2
1	Zn <sub>1.95</sub> Ti <sub>0.95</sub> Cr <sub>0.1</sub> O <sub>4</sub>	900	5.36	2.89	46.2±3.2
1	Zn <sub>1.8</sub> Ti <sub>0.8</sub> Cr <sub>0.4</sub> O <sub>4</sub>	900	5.38	2.41	55.2±3.3
1	Zn <sub>1.5</sub> Ti <sub>0.5</sub> Cr <sub>1.0</sub> O <sub>4</sub>	900	5.45	2.28	58.1±3.5
2 <sup>a</sup>	50ZnO-12.5Cr <sub>2</sub> O <sub>3</sub> -37.5TiO <sub>2</sub>	950	5.21	2.20	57.8±3.5
2 <sup>a</sup>	56.5ZnO-15Cr <sub>2</sub> O <sub>3</sub> -28.5TiO <sub>2</sub>	950	5.28	2.25	57.3±3.4
SA <sup>ab</sup>	50ZnO-25Cr <sub>2</sub> O <sub>3</sub> -25TiO <sub>2</sub>	950	5.26	2.16	58.9±4.1
SA <sup>ab</sup>	60ZnO-15Cr <sub>2</sub> O <sub>3</sub> -25TiO <sub>2</sub>	950	5.30	2.02	62.0±4.3
3 <sup>a</sup>	55ZnO-25Cr <sub>2</sub> O <sub>3</sub> -20TiO <sub>2</sub>	950	5.29	2.14	59.5±4.2
3 <sup>a</sup>	58ZnO- 7Cr <sub>2</sub> O <sub>3</sub> -38TiO <sub>2</sub> <sup>c</sup>	950	5.25	2.49	52.5±3.2

\*data suspected incorrect

<sup>a</sup>all values reported in mole percent

<sup>b</sup>shaded area in Figure 4.3

<sup>c</sup>prepared with ZnO roasted from ZnS

Table 4.3 Crush strength measurements for the Cr-incorporated sorbents.

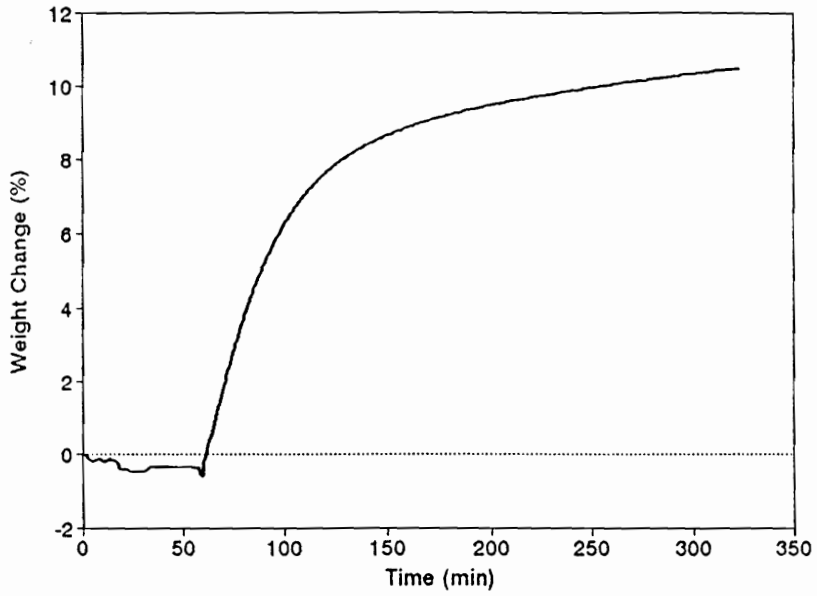
Join	Composition	Sintering <sup>a</sup> Temperature, °C	Crush Strength (N/mm)
1	Zn <sub>1.9</sub> Ti <sub>0.9</sub> Cr <sub>0.2</sub> O <sub>4</sub>	900	112.6±25
1	Zn <sub>1.9</sub> Ti <sub>0.9</sub> Cr <sub>0.2</sub> O <sub>4</sub>	950	119.9±17.2
1	Zn <sub>1.9</sub> Ti <sub>0.9</sub> Cr <sub>0.2</sub> O <sub>4</sub>	1000	163.6±31.2
1	Zn <sub>1.95</sub> Ti <sub>0.95</sub> Cr <sub>0.1</sub> O <sub>4</sub>	900	48.6±12.6*
1	Zn <sub>1.8</sub> Ti <sub>0.8</sub> Cr <sub>0.4</sub> O <sub>4</sub>	900	56.2±12.8*
1	Zn <sub>1.5</sub> Ti <sub>0.5</sub> Cr <sub>1.0</sub> O <sub>4</sub>	900	52.3±7.6
2 <sup>a</sup>	50ZnO-12.5Cr <sub>2</sub> O <sub>3</sub> -37.5TiO <sub>2</sub>	950	72.3±14.3
2 <sup>a</sup>	56.5ZnO-15Cr <sub>2</sub> O <sub>3</sub> -28.5TiO <sub>2</sub>	950	53.6±13.0
SA <sup>a,b</sup>	50ZnO-25Cr <sub>2</sub> O <sub>3</sub> -25TiO <sub>2</sub>	950	37.6±5.0
SA <sup>a,b</sup>	60ZnO-15Cr <sub>2</sub> O <sub>3</sub> -25TiO <sub>2</sub>	950	21.0±4.5
3 <sup>a</sup>	55ZnO-25Cr <sub>2</sub> O <sub>3</sub> -20TiO <sub>2</sub>	950	32.0±9.7
3 <sup>a</sup>	58ZnO- 7Cr <sub>2</sub> O <sub>3</sub> -38TiO <sub>2</sub> <sup>c</sup>	950	126.8±25.4

\*data suspected incorrect

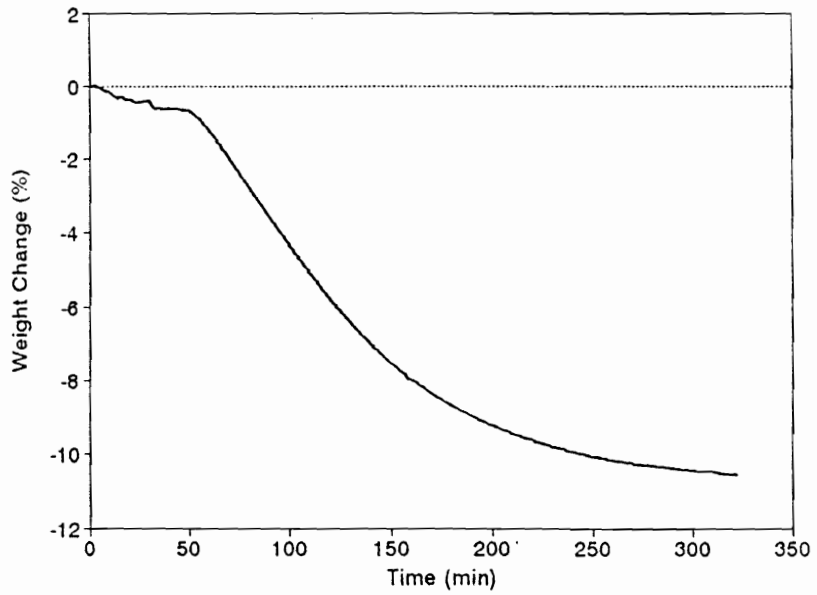
<sup>a</sup>all values reported in mole percent

<sup>b</sup>shaded area in Figure 4.3

<sup>c</sup>prepared with ZnO roasted from ZnS

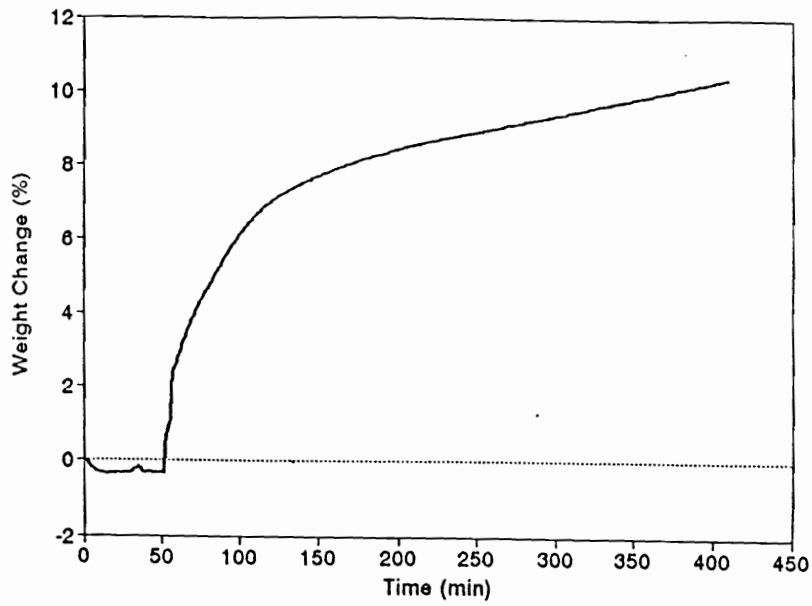


a)

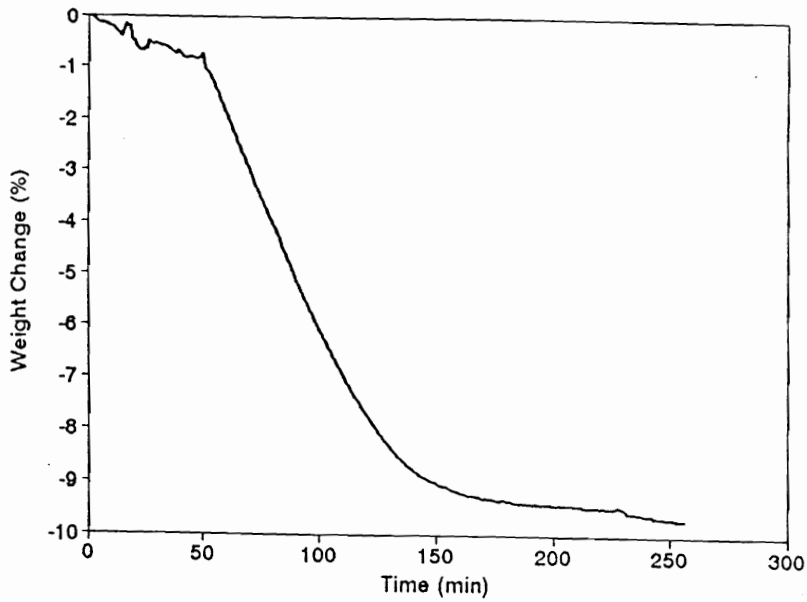


b)

Figure 4.5.  $Zn_{1.9}Ti_{0.9}Cr_{0.2}O_4$  sintered at 900°C for 3 hours a) sulfidation in 0.9%  $H_2S$ , 92.4%  $H_2$ , and 6.7%  $N_2$  at 650°C and b) regeneration in 5%  $O_2$  and 95%  $N_2$  at 650°C.



a)



b)

Figure 4.6.  $Zn_{1.8}Ti_{0.8}Cr_{0.4}O_4$  sintered at  $900^\circ\text{C}$  for 3 hours a) sulfidation in 0.9% $H_2S$ , 92.4% $H_2$ , and 6.7% $N_2$  at  $650^\circ\text{C}$  and b) regeneration in 5% $O_2$  and 95% $N_2$  at  $650^\circ\text{C}$ .

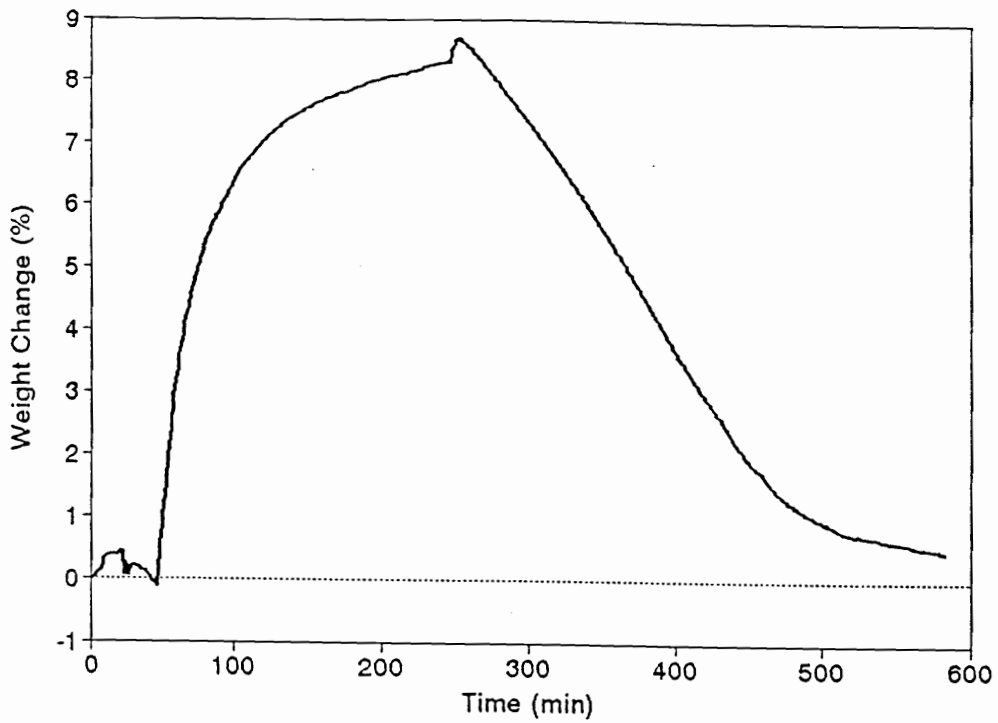


Figure 4.7. Sulfidation in 0.9% $\text{H}_2\text{S}$ , 92.4% $\text{H}_2$ , and 6.7% $\text{N}_2$  at 650°C and regeneration in 5% $\text{O}_2$  and 95% $\text{N}_2$  at 650°C for  $\text{Zn}_{1.95}\text{Ti}_{0.95}\text{Cr}_{0.1}\text{O}_4$  sintered at 900°C for 3 hours.

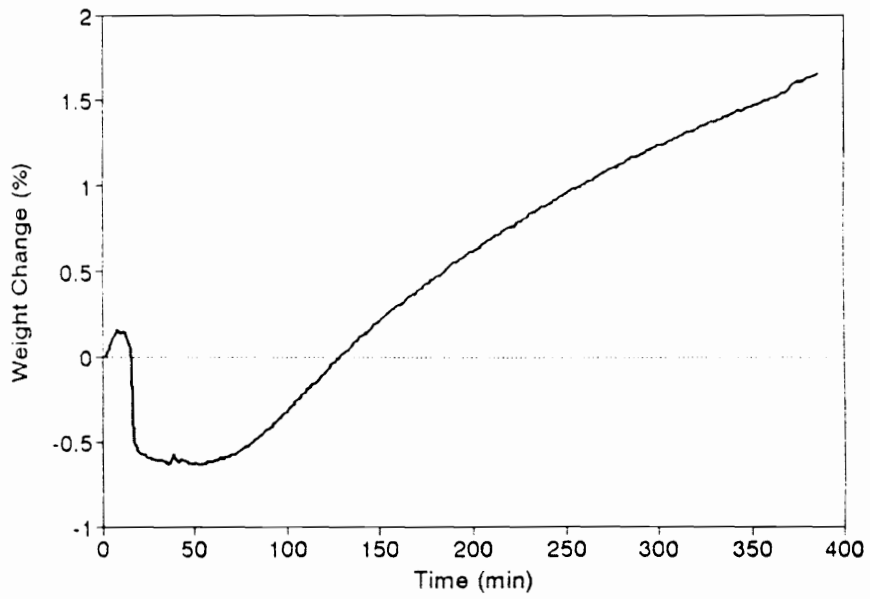
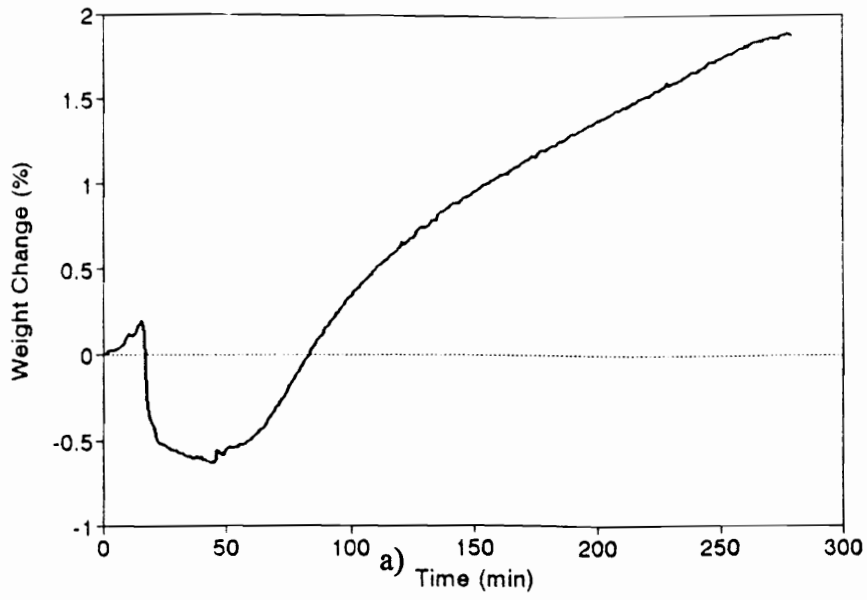
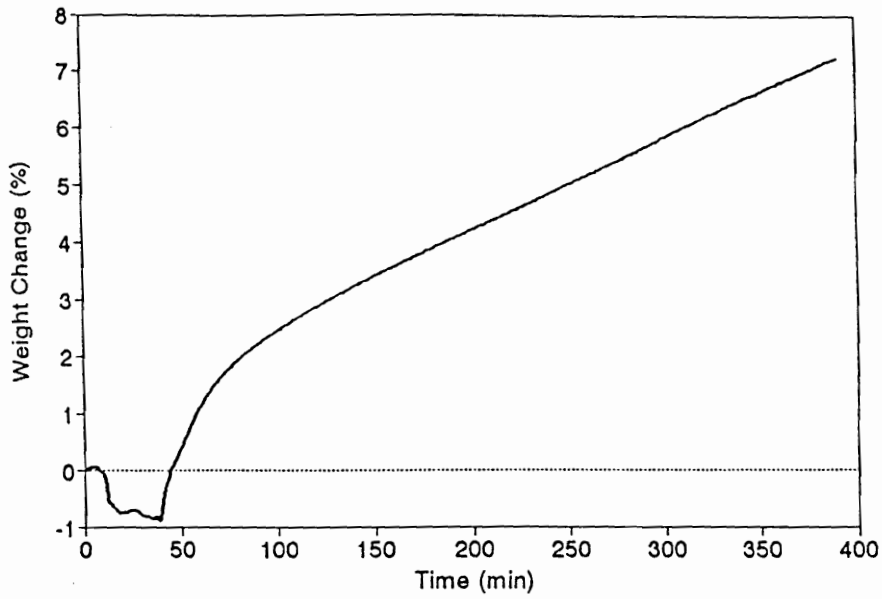


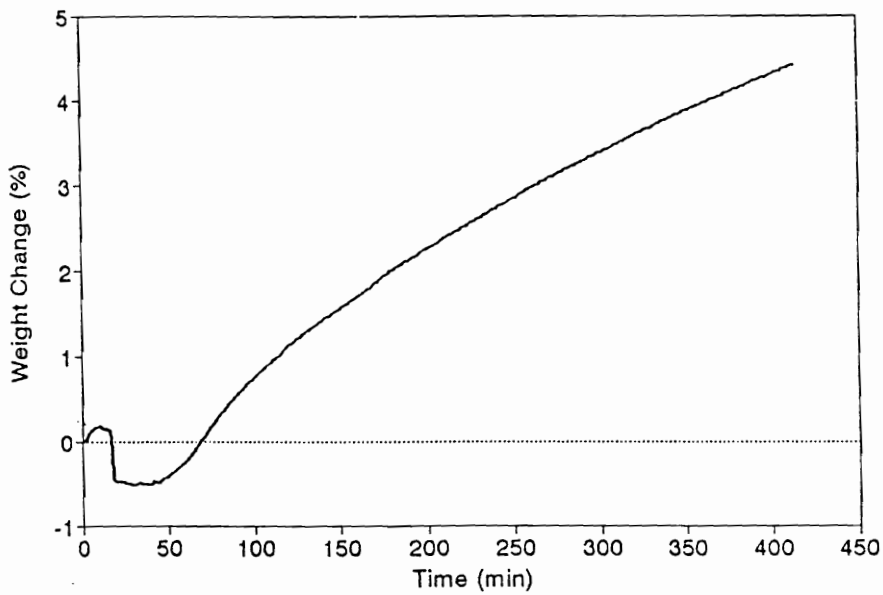
Figure 4.8. Sulfidation in simulated coal gas at 650°C of a) 56.5ZnO-15Cr<sub>2</sub>O<sub>3</sub>-28.5TiO<sub>2</sub> (mole percent) and b) 55ZnO-25Cr<sub>2</sub>O<sub>3</sub>-20TiO<sub>2</sub> (mole percent).

Figure 4.9-4.10 shows TGA curves for  $Zn_{1.6}Cr_{0.4}TiO_{4.2}$  or  $58ZnO-7Cr_2O_3-38TiO_2$ , the composition prepared with the larger particle size ZnO and  $TiO_2$ . This composition was tested in both the  $H_2S$  gas mixture at  $650^\circ C$  and the simulated coal gas at both  $650^\circ C$  and  $725^\circ C$ . At  $650^\circ C$ , there is a large difference in the weight change of the sorbent tested using the two gas compositions. By increasing the testing temperature to  $725^\circ C$ , the weight gain is comparable to that of the  $650^\circ C$  test using the  $H_2S$  mixture.

The weight gain after the sulfidation cycle for all compositions and weight loss for those compositions which were regenerated are listed in Table 4.4. The percent completion of sulfidation, based on the theoretical weight gain of the completely sulfidized  $Zn_2TiO_4$  as a function of Cr incorporation (see Figure 2.2), is also included in this table. As noted above, there is a large difference in the weight change of those samples tested in the  $H_2S$  gas mixture and those tested in simulated coal gas. The reason for this difference is not known. There is twice as much sulfur in the  $H_2S$  mixture than in the simulated coal gas which may have an influence. The porosity of those samples tested in the simulated coal gas are higher than the  $H_2S$  gas mixture ones which should have a positive effect on sulfur removal as there is more surface area exposed. However, the pores may have become blocked during testing or sulfates could have formed which would result in little weight gain. XRD and regeneration data could help explain the poor performance; however, this information is not available for the samples tested in simulated coal gas.



a)



b)

Figure 4.9. 58ZnO-7Cr<sub>2</sub>O<sub>3</sub>-38TiO<sub>2</sub> sintered at 950°C for 3 hours sulfidation in a) simulated coal gas at 650°C and b) 0.9% H<sub>2</sub>S, 92.4% H<sub>2</sub>, and 6.7% N<sub>2</sub> at 650°C.

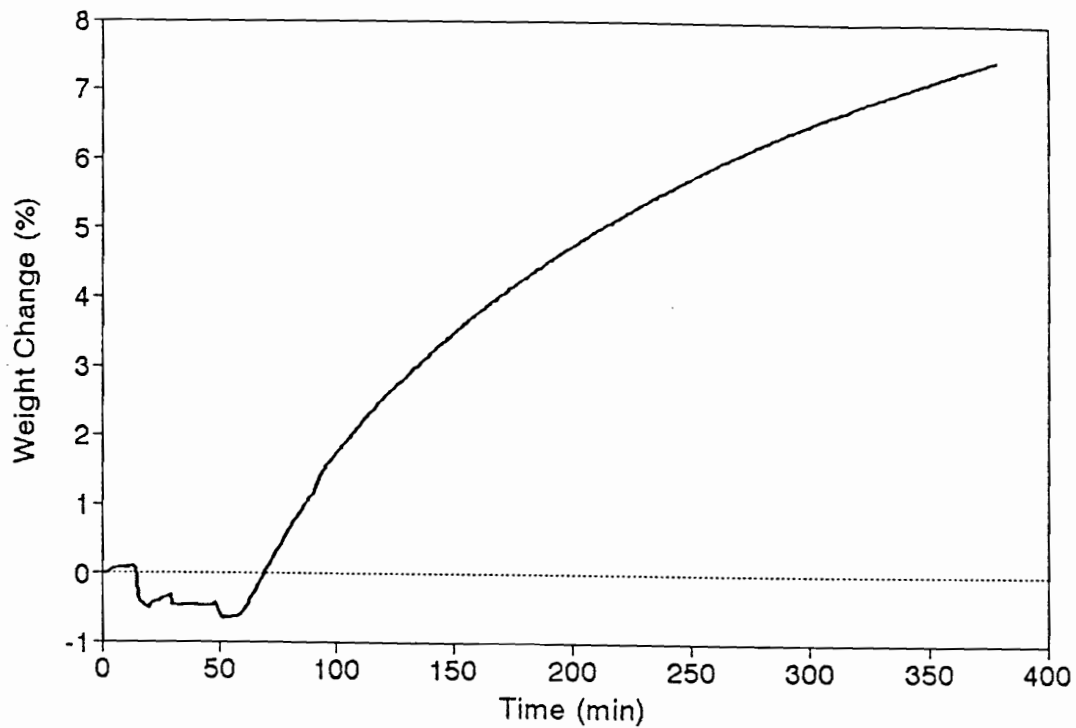


Figure 4.10. Sulfidation of  $58\text{ZnO}-7\text{Cr}_2\text{O}_3-38\text{TiO}_2$  sintered at  $950^\circ\text{C}$  for 3 hours in simulated coal gas at  $725^\circ\text{C}$ .

Table 4.4. Weight change after sulfidation and regeneration TGA tests.

Composition (Sintering Temperature, °C*)	Sulfidation (% Wt. Change)	% Completion of Sulfidation	Regeneration (% Wt. Change)	Gas Composition
Zn <sub>1.9</sub> Ti <sub>0.9</sub> Cr <sub>0.2</sub> O <sub>4</sub> (900) 1st cycle	10.5	71.9	-10.5	H <sub>2</sub> S Mixture
Zn <sub>1.9</sub> Ti <sub>0.9</sub> Cr <sub>0.2</sub> O <sub>4</sub> (900) 2nd cycle	3.0	20.5	-3.0	H <sub>2</sub> S Mixture
Zn <sub>1.9</sub> Ti <sub>0.9</sub> Cr <sub>0.2</sub> O <sub>4</sub> (950)	9.0	61.6	-6.2	H <sub>2</sub> S Mixture
Zn <sub>1.9</sub> Ti <sub>0.9</sub> Cr <sub>0.2</sub> O <sub>4</sub> (1000)	10.2	70.0	-8.0	H <sub>2</sub> S Mixture
Zn <sub>1.95</sub> Ti <sub>0.95</sub> Cr <sub>0.1</sub> O <sub>4</sub> (900)	8.7	62.6	-8.0	H <sub>2</sub> S Mixture
Zn <sub>1.8</sub> Ti <sub>0.8</sub> Cr <sub>0.4</sub> O <sub>4</sub> (900)	10.1	63.1	-10.0	H <sub>2</sub> S Mixture
Zn <sub>1.6</sub> Ti <sub>0.6</sub> Cr <sub>1.0</sub> O <sub>4</sub> (900)	3.0	14.9	NA	Simulated Coal Gas
50ZnO-12.5Cr <sub>2</sub> O <sub>3</sub> -37.5TiO <sub>2</sub> (950) <sup>a</sup>	2.5	13.9	NA	Simulated Coal Gas
56.5ZnO-15Cr <sub>2</sub> O <sub>3</sub> -28.5TiO <sub>2</sub> (950) <sup>a</sup>	2.4	12.3	NA	Simulated Coal Gas
50ZnO-25Cr <sub>2</sub> O <sub>3</sub> -25TiO <sub>2</sub> (950) <sup>a</sup>	2.4	10.4	NA	Simulated Coal Gas
60ZnO-15Cr <sub>2</sub> O <sub>3</sub> -25TiO <sub>2</sub> (950) <sup>a</sup>	3.7	19.5	NA	Simulated Coal Gas
55ZnO-25Cr <sub>2</sub> O <sub>3</sub> -20TiO <sub>2</sub> (950) <sup>a</sup>	2.0	8.3	NA	Simulated Coal Gas
58ZnO- 7Cr <sub>2</sub> O <sub>3</sub> -38TiO <sub>2</sub> (950) <sup>a</sup>	5.0	31.3	NA	Simulated Coal Gas
58ZnO- 7Cr <sub>2</sub> O <sub>3</sub> -38TiO <sub>2</sub> (950) <sup>a</sup>	7.5	46.9	NA	H <sub>2</sub> S Mixture
58ZnO- 7Cr <sub>2</sub> O <sub>3</sub> -38TiO <sub>2</sub> (950) <sup>a</sup> **	8.0	50.0	NA	Simulated Coal Gas

NA = not available

<sup>a</sup>all samples sintered for three hours

<sup>a</sup>all values reported in mole percent

\*\*tested at 725°C, all other samples tested at 650°C

No correlation can be seen between composition and weight gain. Although increasing the amount of Cr in the sorbents should affect the weight gain, see Figure 2.2, the amount of substituted Cr does not appear to be a factor in the performance of the sorbents. No difference was observed between the mode of substitution and the weight gain either; although from the models of substitution suggested in Section 4.2.1 there should be some differences. Substitution mode does not affect the sulfur removal capacity of the sorbent.

#### **4.3.5 TGA from Research Triangle Institute (RTI)**

Several compositions were selected for testing at RTI using TGA to determine the effect of Cr substitution on minimizing zinc losses. The samples were held at the test temperature, 750°C, with no further desulfurization allowed. No reproducible data is available due to inhomogenities within the pellets. This is most probably due to nonuniform distribution of powders during the mixing and pellet preparation.

#### **4.3.6 Semi-quantitative Analysis Using EDX**

Zinc loss during sulfidation has been reported for  $Zn_2TiO_4$  sorbents. [13] One of the goals of this investigation is to reduce the zinc loss through incorporation of refractory cations, such as  $Cr^{3+}$ , into the  $Zn_2TiO_4$  lattice. EDX was used to determine the Zn and Cr content of the sorbents before and after sulfidation. Since vaporization of zinc occurs at the surface of the pellet, analysis was performed only on the surface of the pellet. If there was no Zn loss, the Cr/Zn ratio before and after sulfidation of a sample should remain the

same. A plot of the initial Cr/Zn ratio versus post-sulfidation Cr/Zn ratio would be linear passing through the origin with a slope of 1, Figure 4.11. However, as Zn is lost during sulfidation, the linear plot will move away from the origin with a slope of less than 1. With an increase in Cr<sup>3+</sup> incorporated into the lattice, the loss of zinc is proportionally reduced, and finally reaching a point when the loss is negligible. For example, with a Cr/Zn ratio 0.866 (22.2 mole percent Cr), loss of zinc is ~16%; whereas, increasing the Cr/Zn ratio to 1.85 (43.5 mole percent Cr), the Zn loss is reduced to ~1.2%, see Table 4.5.

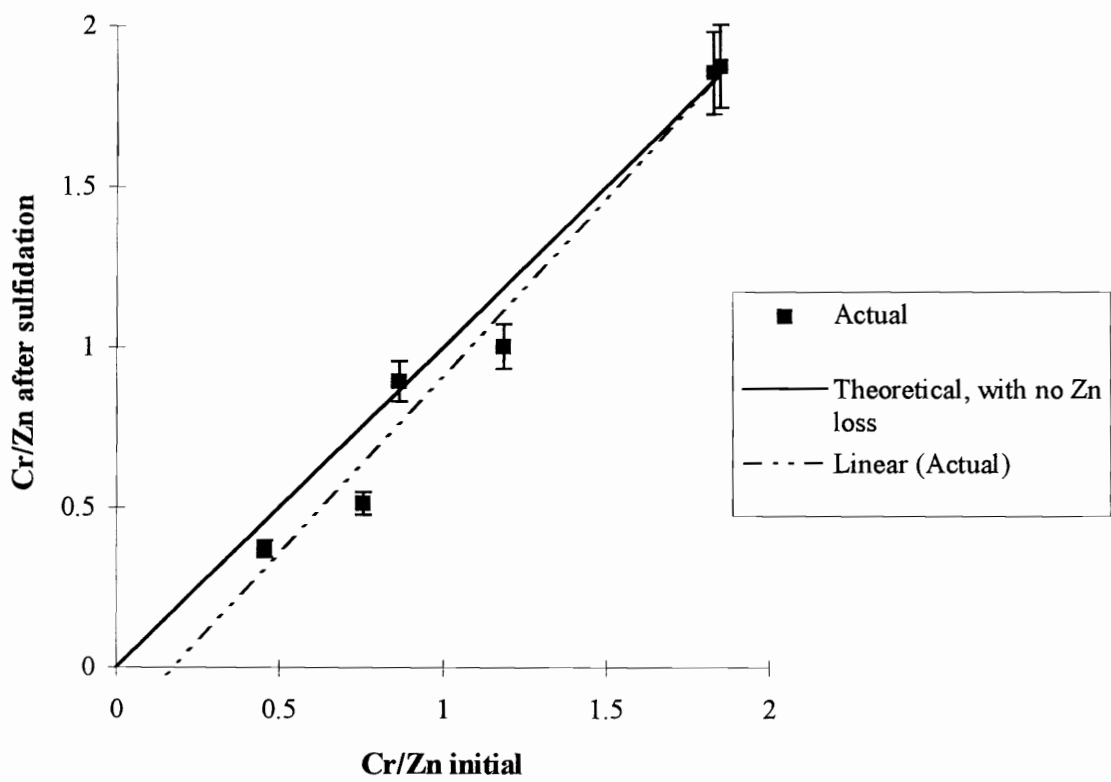


Figure 4.11. Initial Cr/Zn ratio versus Cr/Zn ratio after sulfidation at 650°C for 240 minutes.

Table 4.5 Percent zinc loss after sulfidation of Cr-incorporated Zn<sub>2</sub>TiO<sub>4</sub> sorbents.

Composition	Mole % Cr	Initial Cr/Zn Ratio	Cr/Zn Ratio After Sulfidation	% Zinc Loss
50ZnO-12.5Cr <sub>2</sub> O <sub>3</sub> -37.5TiO <sub>2</sub>	22.2	0.866	0.892	16.4
60ZnO-15 Cr <sub>2</sub> O <sub>3</sub> -25TiO <sub>2</sub>	26.1	1.85	1.872	1.2
50ZnO-25 Cr <sub>2</sub> O <sub>3</sub> -25TiO <sub>2</sub>	40	1.829	1.852	2.3

## 5.0 SUMMARY AND CONCLUSIONS

Mixed metal oxide sorbents are currently being studied for desulfurization of hot coal gas for power generation processes such as the Integrated Gasification Combined Cycle (IGCC). For high efficiency, sorbents should have high sulfur removal capacity, be capable of regenerating back to an oxide, and be durable over many sulfidation and regeneration cycles. Zinc titanate ( $Zn_2TiO_4$ ) based sorbents have more advantages over the other sorbents investigated, such as zinc ferrite and or copper-based sorbents. Zinc titanate sorbents are capable of removing sulfur to less than 10 ppm at high temperatures ( $\sim 700^\circ C$ ); however, they suffer from zinc losses due to vaporization of metallic zinc, low attrition resistance, and physical degradation during the sulfidation and regeneration cycling.

The approach used in this research to eliminate these problems is to modify the composition of  $Zn_2TiO_4$  by incorporating cations into the spinel lattice. The cations were selected after reviewing their potential benefits of improving sulfur removal ability, increasing the attrition resistance, or stabilizing ZnO against Zn vaporization. The first phase of the study consisted of determining the solid solubility of the selected cations in the  $Zn_2TiO_4$  lattice, preliminary screening of the desulfurization performance of the sorbents with various cation concentrations using TGA, and selection of the cation(s) which had the potential for improving  $Zn_2TiO_4$  sorbents. Further testing, including TGA,

EDX, density, porosity, and crush strength measurements, was conducted to determine the effect of cation concentration on the modified  $Zn_2TiO_4$  sorbents.

The following conclusions were observed:

- Various cations (Ni, Cr, Al, Cu, and Mg) can be incorporated in significant amounts in the temperature range from 900 - 1100°C in the  $Zn_2TiO_4$  lattice while still maintaining the spinel structure and properties.
- The preliminary screening experiments indicated that Cr substitution had a beneficial role on improving the performance of  $Zn_2TiO_4$  sorbents over the other selected cations.

Further experiments were conducted to determine how Cr concentration effects the properties of the sorbent. The major observations from the testing are the following:

- Cr-incorporated sorbents, Cr concentration ranging from 3 to 50 mole percent Cr, are stable at 650°C. No exsolution or decomposition of the spinel phases was detected by XRD.
- Crush strength data was inconclusive. However, Cr incorporation does not appear to enhance nor reduce the crush strength of the sorbent.
- Porosity is neither enhanced nor reduced with the additions of Cr in the  $Zn_2TiO_4$  lattice.
- Complete theoretical sulfidation was not achieved for any sample. Several factors which may have caused the incomplete sulfidation are sulfate formation or pore blockage during the sulfidation cycle.

- No correlation can be seen between composition and weight gain. Cr incorporation does not appear to be a factor in sulfur removal.
- Cr-incorporated sorbents reduced Zn losses from 16.4% with 22.2 mole percent Cr to 1.2% loss with 26.1 mole percent Cr.

## REFERENCES

- [1] Yaverbaum, L., *Fluidized Bed Combustion of Coal and Waste Materials*, Noyes Data Corporation, New Jersey, 1977.
- [2] Gangwal, S.K., S.M. Harkins, M.C. Woods, S.C. Jain, and S.J. Bossart, "Bench-Scale Testing of High Temperature Desulfurization Sorbents," *Environ. Prog.*, 8 (4), 265-269, 1989.
- [3] Gangwal, S.K., J.M. Stognar, S.M. Harkins, and S.J. Bossart, "Testing of Novel Sorbents for H<sub>2</sub>S Removal from Coal Gas," *Environ. Prog.*, 8 (1), 26-34, 1989.
- [4] Lew, S., K. Jothimurugesan, and M. Flytzani-Stephanopoulos, "High Temperature H<sub>2</sub>S Removal from Fuel Gases by Regenerable Zinc Oxide-Titanium Dioxide Sorbents," *Ind. Eng. Chem. Res.*, 28 (5), 535-541, 1989.
- [5] Tamhankar, S.S., M. Bagejewicz, G.R. Gavalas, P.K. Sharma, and M. Flytzani-Stephanopoulos, "Mixed Oxide Sorbents for High-Temperature Removal of Hydrogen Sulfide," *Ind. Eng. Chem. Process Des. Dev.*, 25, 429-437, 1986.
- [6] Mojthedi, W., K. Salo, and J. Abbasian, "Desulfurization of Hot Coal Gas in Fluidized-Bed with Regenerable Zinc Titanate Sorbents," *Fuel Proc. Tech.*, 37 (1), 53-65, 1994.
- [7] Westmoreland, P.R., J.B. Gibson, and D.P. Harrison, "Comparative Kinetics of High-Temperature Reaction Between H<sub>2</sub>S and Selected Metal Oxides," *Environ. Sci. Tech.*, 11 (5), 488-491, 1977.
- [8] Westmoreland, P.R. and D.P. Harrison, "Evaluation of Candidate Solids for High-Temperature Desulfurization of Low-Btu Gases," *Environ. Sci. Tech.*, 10 (7), 659-661, 1976.
- [9] Ayala, R.E., E. Gal, S.K. Gangwal, and S.C. Jain, "Enhanced Durability of High-Temperature Desulfurization Sorbents for Moving Bed Applications," *Preprint Papers, Am. Chem. Div. Fuel Chem.*, 35 (1), 120-127, 1990.
- [10] Hower, J.C. and B.K. Parekh, "Chemical/Physical Properties and Marketing," *Coal Preparation*, ed. J. Leonard, Port City Press, Inc., Maryland, 1991.
- [11] Sa, L.N., G.D. Focht, P.V. Ranade, and D.P. Harrison, "High-Temperature Desulfurization Using Zinc Ferrite: Solid Structural Property Changes," *Chem. Eng. Sci.*, 44 (2), 215-224, 1989.

- [12] Sotirchos, S.V. and V.P. Kothari, "Pore Structure and Reactivity Changes in Hot Coal Gas Desulfurization Sorbents," *Proceedings of the Tenth Annual Gasification and Gas Stream Cleanup Systems Contractors Review Meeting*, DOE/METC 90/6115, vol.1, 234-242, 1990.
- [13] Gupta, R.K. and S.K. Gangwal, "Enhanced Durability of Desulfurization Sorbents for Fluidized-Bed Applications," Topical Report, "Development and Testing of Zinc Titanate Sorbents," Research Triangle Institute, NC, work performed under DOE/METC Contract No. DE-AC21-88MC25006, 1992.
- [14] Ayala, R., T. Chuck, E. Gal, and R. Gupta, "Development of Sorbents for High Temperature Desulfurization in Moving Bed Systems," *Proceedings of the Coal-Fired Power Systems 94-Advances in IGCC and PFBC Review Meeting*, vol. II, DOE/METC 94/1008, 637-645, 1994.
- [15] Yates, G. *Fundamentals of Fluidized-bed Chemical Processes*, Butterworths, London, 1983.
- [16] Hypotenuse, Research Triangle Institute, NC, 13, August/September 1989.
- [17] Gupta, R., S.K. Gangwal, and S.C. Jain, "Development of Zinc Ferrite Sorbents for Desulfurization of Hot Coal Gas in a Fluid-Bed Reactor," *Energy and Fuels*, 6 (1), 21-27, 1992.
- [18] Lew, S., A.F. Sarofim, and M. Flytzani-Stephanopoulos, "The Reduction of Zinc Titanate and Zinc Titanate Oxide Solids," *Chem. Eng. Sci.*, 47 (6), 1421-1431, 1992.
- [19] Gangwal, S.K. and S.M. Harkins, "Desulfurization of Hot Coal Gas in a High-Pressure Fluid-Bed Reactor," *Preprint Papers, Am. Chem. Soc. Div. Fuel Chem.*, 35 (1), 161-169, 1990.
- [20] Ayala, R., E. Gal, and S.K. Gangwal, "Enhanced Durability for High-Temperature Desulfurization Sorbents," *Proceedings of the Tenth Annual Gasification and Gas Stream Cleanup Systems Contractors Review Meeting*, DOE/METC 90/6115, vol.1, 112-121, 1990.
- [21] Swisher, J. and K. Schwerdtfeger, "Review of Metals and Binary Oxides as Sorbents for Removing Sulfur from Coal-Derived Gases," *J. Mat. Eng. and Perform.*, 1 (3), 399-407, 1992.
- [22] Ayala, R.E. and D.W. Marsh, "Characterization and Long Range Reactivity of Zinc Ferrite in High-Temperature Desulfurization Processes," *Ind. Eng. Chem. Res.*, 30

(1), 55-60, 1991.

- [23] Flytzani-Stephanopoulos, M. et. al., "Detailed Studies of Novel Regenerable Sorbents for High Temperature Coal Gas Desulfurization," *Proceedings of the Seventh Annual Gasification and Gas Stream Cleanup Systems Contractors Review Meeting*, DOE/METC 87/6019, 1987.
- [24] Gasper-Galvin, L., R. Gupta, and A. Atimay, "Zeolite-Supported Mixed Metal Oxide Sorbents for Hot Gas Desulfurization," unpublished report, 1993.
- [25] Swisher, J. and K. Schwerdtfeger, "Thermodynamic Analysis of Sorption Reactions for the Removal of Sulfur from Hot Gases," *J. Mat. Eng. Perform.*, 1 (4), 565-571, 1992.
- [26] Gasper-Galvin, L., J. Mei, C. Everitt, and S. Katta, "Fixed Bed Testing of Molybdenum-Promoted Zinc Titanate for Hot Gas Desulfurization," prepared for presentation at AIChE Annual Meeting 1993, St. Louis, MO, Paper No. 130g: Gas Purification.
- [27] Gangwal, S.K. and S.C. Jain, "Enhanced Durability of Desulfurization Sorbents for Fluidized-Bed Applications," *Proceedings of the Tenth Annual Gasification and Gas Stream Cleanup Systems Contractors Review Meeting*, DOE/METC 90/6115, vol.1, 102-111, 1990.
- [28] Lercher, J.A., H. Vinek, H. Noller, and J. Stoch, "TiO<sub>2</sub>/ZnO Mixed Oxide Catalysts, Characterization and Infrared Spectroscopy and Reactions with Propanol and Butanol," *Appl. Catal.*, 12 (3), 293-307, 1984.
- [29] Woods, M.C., S.K. Gangwal, K. Jothimurugesan, and D.P. Harrison, "Reaction Between H<sub>2</sub>S and Zinc Oxide-Titanium Dioxide Sorbent. 1. Single Pellet Kinetic Studies," *Ind. Eng. Chem. Res.*, 29, 1160-1167, 1990.
- [30] Swisher, J., W.S. O'Brien, and R. Gupta, "An Attrition Resistant Zinc Titanate Sorbent for Sulfur," Final Report, work performed under DOE Grant No. DE-FC22-PC92521 and Illinois Clean Coal Institute, 1993-1994.
- [31] Focht, G.D., P.V. Ranade, and D.P. Harrison, "High-Temperature Desulfurization Using Zinc Ferrite: Reduction and Sulfidation Kinetics," *Chem. Eng. Sci.*, 43 (11), 3005-3013, 1988.
- [32] Yamaguchi, O., M. Morimi, H. Kawabatha, and K. Shimizu, "Formation and Transformation of ZnTiO<sub>3</sub>," *J. Am. Ceram. Soc.*, 70 (5), C97-C98, 1987.

- [33] Dulin, F.H. and D.E. Rase, "Phase Equilibria in the System ZnO-TiO<sub>2</sub>," *J. Am. Ceram. Soc.*, 43 (3), 125-131, 1959.
- [34] Bartram, S.F. and R.A. Slepety's, "Compound Formation and Crystal Structure in the System ZnO-TiO<sub>2</sub>," *J. Am. Ceram. Soc.*, 44 (9), 493-499, 1961.
- [35] Datta, R.K., "Composition Modification and Characterization of ZnO-TiO<sub>2</sub> Based (ZTB) Desulfurization Sorbents," Final Report, work performed under DOE/METC Contract No. DE-AP21-93MC53415, 1993.
- [36] Datta, R.K. and R. Roy, "Stability of Ni<sub>2</sub>TiO<sub>4</sub>," *Zeit. fur. Kristall.*, Bd. 121, 410-417, 1965.
- [37] Kingery, *Introduction to Ceramics*, John Wiley and Sons, New York, 1976.
- [38] Romeijn, F.C., "Physical and Crystallographical Properties of Some Spinel's I and II," *Philips Res. Rep.*, 8, 304-334, 1953.
- [39] Datta, R.K. and R. Roy, "Equilibrium Order-Disorder in Spinel's," *J. Am. Ceram. Soc.*, 50 (11), 578-583, 1967.
- [40] Muller, O. and R. Roy, *The Major Ternary Structural Families*, Springer-Verlag, New York, 1974.
- [41] Barth, T. and E. Posnjak, "Spinel Structure: With and Without Variate Atom Equipoints," *Zeit. fur Kristall.*, Bd. 82, 325-341, 1932.
- [42] Miller, A., "Distribution of Cations in Spinel's," *J. Appl. Phys. Suppl.*, 30, 245-255, 1959.
- [43] ASTM Index Card.
- [44] Datta, R.K., unpublished data, Virginia Polytechnic Institute and State University, Blacksburg, VA, 1992.
- [45] Newton, G., D. Harrison, and D. Pershing, *Environ. Prog.*, 5 (2), 140-145, 1986.
- [46] Klomp, J., "Physicochemical aspects of ceramic-metal joining," in *Joining of Ceramics*, ed. M. Nichols, Chapman and Hall, New York, 113-127, 1990.
- [47] Yang, J. "Improving the Properties of Zinc Titanate for Sulfur," Ph.d Dissertation, Southern Illinois University at Carbondale, September 1995.

## **APPENDIX A**

<b>Raw Materials</b>	<b>Manufacturer</b>
ZnO	Aldrich Chemical Company
TiO <sub>2</sub>	Aldrich Chemical Company
TiO <sub>2</sub> (2μm mean particle size)	Alfa Products
Cr <sub>2</sub> O <sub>3</sub>	Aldrich Chemical Company
Al <sub>2</sub> O <sub>3</sub>	Fisher Scientific
NiO	Aldrich Chemical Company
MgO	Aldrich Chemical Company
CuO	Aldrich Chemical Company
ACS Reagent Grade Starch	Aldrich Chemical Company
ZnS	Aldrich Chemical Company

## APPENDIX B

### Compositions and Phases Observed During Solid Solubility Experiments

#### System Zn<sub>2</sub>TiO<sub>4</sub> - Ni<sub>2</sub>TiO<sub>4</sub>

Compositions prepared using the general formula Zn<sub>2-x</sub>Ni<sub>x</sub>TiO<sub>4</sub>.

Mole Percent			x	Temperature, °C	Phases Present
ZnO	TiO <sub>2</sub>	NiO			
65.0	33.33	1.67	0.05	1000	(ZnNi) <sub>2</sub> TiO <sub>4</sub> *, ZnO
63.33	33.33	3.33	0.10	900	(ZnNi) <sub>2</sub> TiO <sub>4</sub> , ZnO
				1000	(ZnNi) <sub>2</sub> TiO <sub>4</sub> , ZnO, NiO
61.67	33.33	5.0	0.15	1000	(ZnNi) <sub>2</sub> TiO <sub>4</sub> , ZnO
60.0	33.33	6.67	0.20	900	(ZnNi) <sub>2</sub> TiO <sub>4</sub> , ZnO, NiO, TiO <sub>2</sub>
				1000	(ZnNi) <sub>2</sub> TiO <sub>4</sub> , ZnO
				1100	(ZnNi) <sub>2</sub> TiO <sub>4</sub> , ZnO
58.33	33.33	8.33	0.25	1000	(ZnNi) <sub>2</sub> TiO <sub>4</sub> , ZnO
56.67	33.33	10.0	0.30	900	(ZnNi) <sub>2</sub> TiO <sub>4</sub> , ZnO, NiO, TiO <sub>2</sub>
				1000	(ZnNi) <sub>2</sub> TiO <sub>4</sub> , ZnO, TiO <sub>2</sub>
				1100	(ZnNi) <sub>2</sub> TiO <sub>4</sub> , ZnO
53.33	33.33	10.33	0.40	900	(ZnNi) <sub>2</sub> TiO <sub>4</sub> , ZnO, NiO, TiO <sub>2</sub>
				1000	(ZnNi) <sub>2</sub> TiO <sub>4</sub> , ZnO, TiO <sub>2</sub>
				1100	(ZnNi) <sub>2</sub> TiO <sub>4</sub> , ZnO
50.0	33.33	16.67	0.50	1000	(ZnNi) <sub>2</sub> TiO <sub>4</sub> , ZnO, TiO <sub>2</sub>
				1100	(ZnNi) <sub>2</sub> TiO <sub>4</sub> , ZnO, TiO <sub>2</sub>
46.67	33.33	20.0	0.60	900	(ZnNi) <sub>2</sub> TiO <sub>4</sub> , ZnO, NiO, TiO <sub>2</sub>
				1000	(ZnNi) <sub>2</sub> TiO <sub>4</sub> , ZnO, NiO, TiO <sub>2</sub>
				1100	(ZnNi) <sub>2</sub> TiO <sub>4</sub>
43.33	33.33	23.33	0.70	900	(ZnNi) <sub>2</sub> TiO <sub>4</sub> , ZnO, NiO, TiO <sub>2</sub>
				1000	(ZnNi) <sub>2</sub> TiO <sub>4</sub> , ZnO, NiO, TiO <sub>2</sub>
				1100	(ZnNi) <sub>2</sub> TiO <sub>4</sub> , TiO <sub>2</sub>
33.33	33.33	33.33	1.0	900	(ZnNi) <sub>2</sub> TiO <sub>4</sub> , ZnO, NiO, TiO <sub>2</sub>
				1000	(ZnNi) <sub>2</sub> TiO <sub>4</sub> , ZnO, NiO, TiO <sub>2</sub>
				1100	(ZnNi) <sub>2</sub> TiO <sub>4</sub> , NiO, TiO <sub>2</sub>
26.67	33.33	40.0	1.2	900	(ZnNi) <sub>2</sub> TiO <sub>4</sub> , ZnO, NiO, TiO <sub>2</sub>
				1000	(ZnNi) <sub>2</sub> TiO <sub>4</sub> , ZnO, NiO, TiO <sub>2</sub>
				1100	(ZnNi) <sub>2</sub> TiO <sub>4</sub> , ZnO, NiO, TiO <sub>2</sub>

\*spinel solid solution phase

System Zn<sub>2</sub>TiO<sub>4</sub> - ZnCr<sub>2</sub>O<sub>4</sub>

Compositions prepared using the general formula Zn<sub>2-x</sub>Ti<sub>1-x</sub>Cr<sub>2x</sub>O<sub>4</sub>.

Mole Percent			x	Temperature, °C	Phases Present
ZnO	TiO <sub>2</sub>	Cr <sub>2</sub> O <sub>3</sub>			
65.0	31.67	3.33	0.05	900	(ZnTiCr) <sub>3</sub> O <sub>4</sub> *, ZnO, Cr <sub>2</sub> O <sub>3</sub>
				1000	(ZnTiCr) <sub>3</sub> O <sub>4</sub>
63.33	30.0	6.67	0.10	900	(ZnTiCr) <sub>3</sub> O <sub>4</sub> , ZnO
				1000	(ZnTiCr) <sub>3</sub> O <sub>4</sub>
				1100	(ZnTiCr) <sub>3</sub> O <sub>4</sub>
61.67	28.33	10.0	0.15	900	(ZnTiCr) <sub>3</sub> O <sub>4</sub> , ZnO, TiO <sub>2</sub>
				1000	(ZnTiCr) <sub>3</sub> O <sub>4</sub>
				1100	(ZnTiCr) <sub>3</sub> O <sub>4</sub>
60.0	26.67	13.33	0.20	900	(ZnTiCr) <sub>3</sub> O <sub>4</sub> , ZnO, TiO <sub>2</sub>
				1000	(ZnTiCr) <sub>3</sub> O <sub>4</sub> , ZnO, TiO <sub>2</sub>
				1100	(ZnTiCr) <sub>3</sub> O <sub>4</sub>
58.33	25.0	16.67	0.25	900	(ZnTiCr) <sub>3</sub> O <sub>4</sub> , ZnO, TiO <sub>2</sub> , Cr <sub>2</sub> O <sub>3</sub>
				1000	(ZnTiCr) <sub>3</sub> O <sub>4</sub> , TiO <sub>2</sub> , Cr <sub>2</sub> O <sub>3</sub>
				1100	(ZnTiCr) <sub>3</sub> O <sub>4</sub>
56.67	23.33	20.0	0.30	900	(ZnTiCr) <sub>3</sub> O <sub>4</sub> , ZnO, TiO <sub>2</sub>
				1000	(ZnTiCr) <sub>3</sub> O <sub>4</sub> , TiO <sub>2</sub> , Cr <sub>2</sub> O <sub>3</sub>
				1100	(ZnTiCr) <sub>3</sub> O <sub>4</sub> , TiO <sub>2</sub>
53.33	20.0	26.67	0.40	900	(ZnTiCr) <sub>3</sub> O <sub>4</sub> , ZnO, TiO <sub>2</sub> , Cr <sub>2</sub> O <sub>3</sub>
				1000	(ZnTiCr) <sub>3</sub> O <sub>4</sub> , ZnO, TiO <sub>2</sub>
				1100	(ZnTiCr) <sub>3</sub> O <sub>4</sub> , TiO <sub>2</sub>
50.0	16.67	33.33	0.50	900	(ZnTiCr) <sub>3</sub> O <sub>4</sub> , ZnO, TiO <sub>2</sub> , Cr <sub>2</sub> O <sub>3</sub>
				1000	(ZnTiCr) <sub>3</sub> O <sub>4</sub> , TiO <sub>2</sub>
				1100	(ZnTiCr) <sub>3</sub> O <sub>4</sub> , TiO <sub>2</sub>

\*spinel solid solution phase

System Zn<sub>2</sub>TiO<sub>4</sub> - ZnAl<sub>2</sub>O<sub>4</sub>

Compositions prepared using the general formula Zn<sub>2-x</sub>Ti<sub>1-x</sub>Al<sub>2x</sub>O<sub>4</sub>.

Mole Percent			x	Temperature, °C	Phases Present
ZnO	TiO <sub>2</sub>	Al <sub>2</sub> O <sub>3</sub>			
65.0	31.67	3.33	0.05	900	(ZnTiAl) <sub>3</sub> O <sub>4</sub> *, ZnO, Al <sub>2</sub> O <sub>3</sub>
				1000	(ZnTiAl) <sub>3</sub> O <sub>4</sub> , ZnO, Al <sub>2</sub> O <sub>3</sub>
63.33	30.0	6.67	0.10	900	(ZnTiAl) <sub>3</sub> O <sub>4</sub> , ZnO, Al <sub>2</sub> O <sub>3</sub>
				1000	(ZnTiAl) <sub>3</sub> O <sub>4</sub> , ZnO, TiO <sub>2</sub> , Al <sub>2</sub> O <sub>3</sub>
				1100	(ZnTiAl) <sub>3</sub> O <sub>4</sub> , ZnO, TiO <sub>2</sub> , Al <sub>2</sub> O <sub>3</sub>
61.67	28.33	10.0	0.15	900	(ZnTiAl) <sub>3</sub> O <sub>4</sub> , ZnO, Al <sub>2</sub> O <sub>3</sub>
				1000	(ZnTiAl) <sub>3</sub> O <sub>4</sub> , ZnO, TiO <sub>2</sub>
				1100	(ZnTiAl) <sub>3</sub> O <sub>4</sub> , TiO <sub>2</sub>
60.0	26.67	13.33	0.20	900	(ZnTiAl) <sub>3</sub> O <sub>4</sub> , ZnO, Al <sub>2</sub> O <sub>3</sub>
				1000	(ZnTiAl) <sub>3</sub> O <sub>4</sub> , ZnO, TiO <sub>2</sub> , Al <sub>2</sub> O <sub>3</sub>
				1100	(ZnTiAl) <sub>3</sub> O <sub>4</sub> , ZnO, TiO <sub>2</sub>
58.33	25.0	16.67	0.25	900	(ZnTiAl) <sub>3</sub> O <sub>4</sub> , ZnO, Al <sub>2</sub> O <sub>3</sub>
				1000	(ZnTiAl) <sub>3</sub> O <sub>4</sub> , ZnO, Al <sub>2</sub> O <sub>3</sub>
				1100	(ZnTiAl) <sub>3</sub> O <sub>4</sub> , ZnO
56.67	23.33	20.0	0.30	900	(ZnTiAl) <sub>3</sub> O <sub>4</sub> , ZnO, Al <sub>2</sub> O <sub>3</sub>
				1000	(ZnTiAl) <sub>3</sub> O <sub>4</sub> , ZnO, Al <sub>2</sub> O <sub>3</sub>
				1100	(ZnTiAl) <sub>3</sub> O <sub>4</sub> , ZnO
53.33	20.0	26.67	0.40	900	(ZnTiAl) <sub>3</sub> O <sub>4</sub> , ZnO, Al <sub>2</sub> O <sub>3</sub>
				1000	(ZnTiAl) <sub>3</sub> O <sub>4</sub> , ZnO, TiO <sub>2</sub> , Al <sub>2</sub> O <sub>3</sub>
				1100	(ZnTiAl) <sub>3</sub> O <sub>4</sub> , ZnO, TiO <sub>2</sub> , Al <sub>2</sub> O <sub>3</sub>
50.0	16.67	33.33	0.50	900	(ZnTiAl) <sub>3</sub> O <sub>4</sub> , ZnO, Al <sub>2</sub> O <sub>3</sub>
				1000	(ZnTiAl) <sub>3</sub> O <sub>4</sub> , ZnO, Al <sub>2</sub> O <sub>3</sub>
				1100	(ZnTiAl) <sub>3</sub> O <sub>4</sub> , TiO <sub>2</sub> , Al <sub>2</sub> O <sub>3</sub>

\*spinel solid solution phase

System  $Zn_2TiO_4$  -  $Mg_2TiO_4$

Compositions prepared using the general formula  $Zn_{2-x}Mg_xTiO_4$ .

Mole Percent			x	Temperature, °C	Phases Present
ZnO	TiO <sub>2</sub>	MgO			
58.33	33.33	8.33	0.25	900	(ZnMg) <sub>2</sub> TiO <sub>4</sub> *, ZnTiO <sub>3</sub> , ZnO
				1000	(ZnMg) <sub>2</sub> TiO <sub>4</sub> , ZnO, MgO
				1100	(ZnMg) <sub>2</sub> TiO <sub>4</sub> , ZnO
50.0	33.33	16.67	0.50	900	(ZnMg) <sub>2</sub> TiO <sub>4</sub> , ZnTiO <sub>3</sub> , ZnO, MgO
				1000	(ZnMg) <sub>2</sub> TiO <sub>4</sub> , ZnTiO <sub>3</sub> , ZnO, MgO
				1100	(ZnMg) <sub>2</sub> TiO <sub>4</sub> , ZnO
41.67	33.33	25.0	0.75	900	(ZnMg) <sub>2</sub> TiO <sub>4</sub> , ZnTiO <sub>3</sub> , ZnO, MgO
				1000	(ZnMg) <sub>2</sub> TiO <sub>4</sub> , ZnTiO <sub>3</sub> , ZnO, MgO
				1100	(ZnMg) <sub>2</sub> TiO <sub>4</sub> , ZnTiO <sub>3</sub> , ZnO
33.33	33.33	33.33	1.0	900	(ZnMg) <sub>2</sub> TiO <sub>4</sub> , ZnTiO <sub>3</sub> , ZnO, MgO
				1000	(ZnMg) <sub>2</sub> TiO <sub>4</sub> , ZnTiO <sub>3</sub> , ZnO, MgO
				1100	(ZnMg) <sub>2</sub> TiO <sub>4</sub> , ZnTiO <sub>3</sub> , ZnO, MgO

\*spinel solid solution phase

System Zn<sub>2</sub>TiO<sub>4</sub> - Cu<sub>2</sub>TiO<sub>4</sub>

Compositions prepared using the general formula Zn<sub>2-x</sub>Cu<sub>x</sub>TiO<sub>4</sub>.  
(fired in alumina crucibles)

Mole Percent			x	Temperature, °C	Phases Present
ZnO	TiO <sub>2</sub>	CuO			
58.33	33.33	8.33	0.25	900	(ZnCu) <sub>2</sub> TiO <sub>4</sub> *, ZnO, CuTiO <sub>x</sub> **, TiO <sub>2</sub>
				1000	(ZnCu) <sub>2</sub> TiO <sub>4</sub> , ZnO, CuTiO <sub>x</sub>
				1100	(ZnCu) <sub>2</sub> TiO <sub>4</sub> , ZnO, CuTiO <sub>x</sub>
50.00	33.33	16.67	0.50	900	(ZnCu) <sub>2</sub> TiO <sub>4</sub> , ZnO, CuTiO <sub>x</sub> , TiO <sub>2</sub>
				1000	(ZnCu) <sub>2</sub> TiO <sub>4</sub> , ZnO, CuTiO <sub>x</sub>
41.67	33.33	25.0	0.75	900	(ZnCu) <sub>2</sub> TiO <sub>4</sub> , ZnO, CuTiO <sub>x</sub> , TiO <sub>2</sub>
				33.33	33.33
0	33.33	66.67	2.0	900	CuO, TiO <sub>2</sub> , CuTiO <sub>x</sub>

\*spinel solid solution phase

\*\*Cu<sub>2</sub>TiO<sub>5</sub> or Cu<sub>2</sub>TiO<sub>3</sub>

System Zn<sub>2</sub>TiO<sub>4</sub> - Cu<sub>2</sub>TiO<sub>4</sub>

Compositions prepared using the general formula Zn<sub>2-x</sub>Cu<sub>x</sub>TiO<sub>4</sub>.  
(fired in platinum crucibles)

Mole Percent			x	Temperature, °C	Phases Present
ZnO	TiO <sub>2</sub>	CuO			
58.33	33.33	8.33	0.25	1000	(ZnCu) <sub>2</sub> TiO <sub>4</sub> , CuTiO <sub>x</sub> **
				1100	(ZnCu) <sub>2</sub> TiO <sub>4</sub> , CuTiO <sub>x</sub> , ZnO
50.0	33.33	16.67	0.50	1000	(ZnCu) <sub>2</sub> TiO <sub>4</sub> , CuTiO <sub>x</sub>
				1100	(ZnCu) <sub>2</sub> TiO <sub>4</sub> , CuTiO <sub>x</sub>
41.67	33.33	25.0	0.75	1000	(ZnCu) <sub>2</sub> TiO <sub>4</sub> , CuTiO <sub>x</sub> , ZnO
				1100	(ZnCu) <sub>2</sub> TiO <sub>4</sub> , CuTiO <sub>x</sub> , ZnO
33.33	33.33	33.33	1.0	1000	(ZnCu) <sub>2</sub> TiO <sub>4</sub> , ZnO, CuO

\*spinel solid solution phase

\*\*Cu<sub>2</sub>TiO<sub>5</sub> or Cu<sub>2</sub>TiO<sub>3</sub>

## APPENDIX C

### Sample Calculation of Theoretical Density



$$a_0 = 8.437 = 8.437 \times 10^{-8} \text{ cm (determined from XRD)}$$

$$V = a_0^3 = 6.0057 \times 10^{-22} \text{ cm}^3$$

$$\begin{aligned} M &= 1.9(65.37 \text{ g/mol}) + 0.9(47.9 \text{ g/mol}) + 0.2(51.996 \text{ g/mol}) + 4(16 \text{ g/mol}) \\ &= 241.734 \text{ g/mol} \end{aligned}$$

$$\rho_0 = 8 \text{ MN/V}$$

N = Avagadro's Number

$$\rho_0 = \frac{8 (241.734 \text{ g/mol} / 6.023 \times 10^{23} \text{ mol})}{(6.0057 \times 10^{-22} \text{ cm}^3)}$$

$$\rho_0 = 5.35 \text{ g/cm}^3$$

## VITA

Kimberly Walton was born in Kansas City, Missouri on July 23, 1971. She graduated from Green Run High School in Virginia Beach, Virginia in 1989. In August, 1989, she began studying at Virginia Polytechnic Institute and State University and graduated with a Bachelor of Science in Materials Science and Engineering in May, 1993. She started graduate school at VPI & SU in August, 1993. In September, 1995, she completed the requirements for a Master of Science.

*Kimberly S. Walton*